
Multi-data Image Fusion for Mapping the Wetland Vegetation in Poyang Lake, China

by

Zhuoya Ji

This thesis submitted to the International Institute for Geo-information Science and Earth Observation (The Netherlands) and the School of Resource and Environment Science (SRES) of Wuhan University (China) in partial fulfilment of the requirements for the degree of Master of Science in Geo-information Science and Earth Observation, Specialisation: Natural Resources Management.

Thesis Assessment Board

Prof. Dr. Ir. Alfred de Gier, Chairman (ITC)
Prof. Liu Xuehua, External Examiner (Tsinghua University)
Dr. Michael Weir, Course Director (ITC)
Prof. Dr. He Zongyi, Supervisor (SRES)

Supervisors: Dr. Yousif Hussin (ITC), Prof. Dr. He Zongyi (SRES)



**INTERNATIONAL INSTITUTE FOR GEO-INFORMATION SCIENCE AND EARTH OBSERVATION
ENSCHDE, THE NETHERLANDS
SHOOL OF RESOURCES AND ENVIRONMENTAL SCIENCE (SRES)
WUHAN UNIVERSITY, CHINA**

Disclaimer

This document describes work undertaken as part of a programme of study at the International Institute for Geo-information Science and Earth Observation. All views and opinions expressed therein remain the sole responsibility of the author, and do not necessarily represent those of the institute.

Abstract

Wetlands are decreasing worldwide at a shocking speed due to human activities. With the development of remote sensing and geographic information systems, management of wetlands based on monitoring vegetation communities has become efficient comparing to costly and slow field survey. However, optical remote sensing can not always adequately discriminate between wetland vegetation communities. Additionally, the typically humid weather of wetlands reduces the quality and quantity of optical satellite imagery, which is already difficult to obtain in developing countries. As a solution, this research investigates the fusion of optical and radar imagery, which are expect to have complimentary information. The aim of this study is to determine the success of two image fusion techniques, Brovey and Intensity, Hue and Saturation (IHS) transformation, in identifying wetland vegetation communities. Prior to image fusion, maximum likelihood classification of wetland communities (*Carex*, *Miscanthus* and *Cynodon*) was done separately for ALOS optical and ENVISAT radar imagery. Classification of ALOS imagery was able to discriminate grassland communities (overall accuracy 88.7%, kappa 0.86), albeit with some misclassification. Three vegetation classes were distributed in a belt shape around the lake, but it was hard to tell which of *Carex* and *Miscanthus* was closer to the lake. Sand was easily-identifiable. Classification of ENVISAT imagery could barely separate three vegetation communities (overall accuracy 75%, kappa 0.66), although the water bodies were defined well. Most of the sand cover area was misclassified into water class. Classification of both fused images was more successful. Sand and water classes were totally separated in both fused classifications. In the Brovey result map (overall accuracy 93.4%, kappa 0.91), the *Miscanthus* community was mapped as scattered areas rather than a belt shape. Yet, it was still obvious that *Carex* was closest to the lake, followed by *Miscanthus*, and *Cynodon*. These three vegetation communities separated very well in the IHS map (overall accuracy 94.4%, kappa 0.93). Multisensor image fusion, taking advantage of the complimentary information content, was able to successfully map wetland vegetation communities. The potential for cheap and timely monitoring for effective management is clear.

Key words: wetland, vegetation community, image fusion, Brovey Transformation, IHS Transformation, remote sensing, ALOS, ENVISAT radar

Acknowledgements

On the completion of my MSc thesis, I would like to express my deepest gratitude to all those people whose kindness and advice have made this work possible.

Firstly, as an exchange student, I want to thank the International Institute for Geo-Information Science and Earth Observation (ITC) and Wuhan University for providing me such precious chance to live and study abroad in the Netherlands. I have learned a lot and opened my eyes to the world because of this valuable experience.

I am greatly indebted to my supervisor Prof. Yousif Hussin, who gave me valuable instructions in this research and even came to Poyang Lake in China to support our field work academically and materially. His effective advice, shrewd comments have kept the thesis in the right direction. With his great help, I finally overcame the problems in the research one by one. I also want to express my deep appreciation to my second supervisor Prof. He Zongyi. Thank you for your persistent concern and support to my research and always give me inspiring ideas during the whole time.

My special thanks go to Pro. David Rossiter, a respectable, responsible and resourceful scholar, who has provided me with valuable guidance in the stage of writing this thesis. Thanks very much to Prof. Jan De Leeuw who help me to conceive this topic in the first place and hep me to acquire data for the research. To Programme Director Prof. Michael Wier, I give my sincere appreciation to you for your continuous help in my study life even before I came to the Netherlands.

I am grateful to Mr Wang Tiejun and Ms. Si Yali for the permanent help and priceless suggestion in my study. They clarified so many problems I met in the process of conduct this research for me. Many thanks to Mr Wu Guofeng, I appreciate a lot for your continuous critical suggestion in my research. Many thanks go to Prof. Du Qingyun for his arrangement of the field work.

To Mr. Li Wei who works at Institute of Botany in Wuhan Botany Garden, I want to express my thanks. With his instruction, we understand the basic issue of vegetation field survey. I am grateful to the staff of Natural Reserve of Poyang Lake who offered me great help in the field.

I would like to thank my partner Xu Chonglin for her company during the field work and other girls in our team, Liu Miwei, Zhou Xichang and Zeng Rong. They constantly encouraged me when I felt frustrated with this dissertation. Thank you for your constructive suggestions and made my life colourful in the foreign country.

In the end and I would like to express my eternal appreciation to my parents. Thank you for provide such precious opportunity to study in ITC and support me for every difficulty in my life!

Table of contents

Abstract	i
Acknowledgements.....	ii
List of figures	v
List of tables.....	vi
1. Introduction.....	1
1.1. Background	1
1.2. Problem Statement and Justification	1
1.3. Research Objective	4
1.4. Research Questions.....	4
1.5. Research Hypothesis.....	4
1.6. Outline of the Thesis	4
2. Materials and methods	6
2.1. Study area	6
2.2. Research materials.....	8
2.2.1. Field data	8
2.2.2. Satellite Imagery and Ancillary Data.....	8
2.3. Research Methods.....	10
2.3.1. Field Survey	11
2.3.1.1. Sample design	11
2.3.1.2. Field data collection.....	12
2.3.2. Satellite data preprocessing.....	13
2.3.2.1. Radiometric Correction.....	13
2.3.2.2. Geometric Correction and Rectification.....	14
2.3.2.3. Image subset	15
2.3.3. Image Fusion.....	16
2.3.4. Image Classification	17
2.3.5. Accuracy Assessment	17
2.3.6. Testing for a Significant Difference between Images.....	18
3. Results and Discussion.....	19
3.1. Single Images	19
3.1.1. ALOS Optical Image.....	19
3.1.2. ENVISAT Radar Image	19
3.2. Fused Images.....	21
3.2.1. Brovey Transformation.....	21
3.2.2. Intensity Hue and Saturation (IHS)	23
3.3. Classification Results.....	24
3.3.1. Training and Validating Samples	24
3.3.2. Single image mapping.....	25

3.3.3.	Fused image mapping.....	27
3.3.4.	Classification Accuracy Assessment and Comparison	29
3.3.5.	Test of Significance.....	35
4.	Conclusion and Recommendations.....	37
4.1.	Conclusions.....	37
4.2.	Implementation.....	38
4.3.	Concluding Remarks	38
4.4.	Recommendations.....	39
	References.....	41
	Appendix: Radar filters.....	44

List of figures

Figure 1 Location of Poyang Lake	6
Figure 4 Framework of the research.....	10
Figure 5 Location of field samples.....	11
Figure 6 Field work activities (a. measure height of vegetation community; b. cut vegetation above the ground; c. one example of 30x30cm square frame after all the vegetation was cut; d. weight the fresh biomass of one 30x30cm square frame)	13
Figure 7 ALOS optical image (band 4, 2, 1 assigned to red, green and blue) of the study area	20
Figure 8 ENVISAT ASAR Radar (VV-polarized) of the study area.....	20
Figure 9 Result of Brovey Transformation technique applied to ALOS and radar images ...	21
Figure 10 Radar returns as a function of geometric properties of object (Lillesand and Kiefer, 1994)	22
Figure 11 Result of Intensity Hue and Saturation (IHS) technique applied to ALOS and radar images	23
Figure 12 Classified image of ALOS.....	25
Figure 13 Classification map of the ENVISAT Radar image.....	26
Figure 14 Brovey Transformation image fusion mapping	27
Figure 15 IHS Transformation image fusion mapping	28
Figure 16 Comparison of single images and transformation images by overall accuracy and Kappa statistic	33
Figure 17 Producers accuracy and Kappa statistic of three vegetation communities with both unfused and fused images	34
Figure 18 Users accuracy and Kappa statistic of three vegetation communities with both unfused and fused images	34

List of tables

Table 1 Training and validating sample for maximum likelihood classification	24
Table 2 Error matrix for supervised classification of ALOS optical imagery	29
Table 3 Accuracy assessment for supervised classification of ALOS optical imagery	29
Table 4 Error matrix for supervised classification of ENVISAT Radar imagery	30
Table 5 Accuracy assessment for supervised classification of ENVISAT Radar imagery	30
Table 6 Error matrix for supervised classification of fused image using Brovey Transformation technique	31
Table 7 Accuracy assessment for supervised classification of fused image using Brovey Transformation technique	31
Table 8 Error matrix for supervised classification of fused image using IHS Transformation technique.....	32
Table 9 Accuracy assessment for supervised classification of fused image using IHS Transformation technique	32
Table 10 Accuracy comparison between three vegetation communities with single image (ALOS and radar) classification map and fused image (Brovey and IHS) classification map	35
Table 11 Test of Significant difference between single data classified images and fused data classified images.....	36

1. Introduction

1.1. Background

Wetland, as an important environment, is at the interface between terrestrial ecosystems and aquatic systems which make them essentially different from each other yet greatly dependent on each other too (Mitsch and Gosselink, 2000). It is considered one of the most indispensable ecosystems on earth, which provides critical nesting, rearing, feeding and stopover habitat for millions of water birds, fish and other wildlife (Dugan, 1991). Besides its ecosystem value, wetland also fulfills crucial ecological functions, which include recharging ground water, cycling nutrient, preventing flood and erosion, controlling sediments and cleaning polluted water and storing surface and subsurface water (Dugan, 1991; Simonit et al., 2005).

In spite of the wide importance ranging from economic, social, recreational, a scientific and cultural perspective, the speed of disappearance of these unique ecosystems is shocking (at global level) as a consequence of human activities (Mitsch and Gosselink, 2000). This is because of the booming population, the human demand for resources is increasing through time, which leads to their aggressive intervention in wetlands.

Contributing 10 percent to the world's total area of wetland, China use to have 650,000 km² of this type of ecosystem, which was the largest in Asia and the fourth largest in the world (CTAL., 2006). However, due to the excessive cultivation in China's largest marshland area in Sanjing (Three Rivers) plain, during the last several decades, only 380,000 km² of those wetlands are still exist (Chen, 2007). Moreover, with decades of embankment and reclamation for cultivation, the disastrous floods in the summer of 1998 had seriously damaged wetland in Poyang Lake and Dongting Lake which located along the Yangtze River (XNA., 2006). Therefore, future generations feel responsible to sustainably manage these wetland resources. Also they feel that protecting and restoring wetland in China is an extremely urgent issue.

1.2. Problem Statement and Justification

Since wetland vegetation could accumulates sediments and organic matter, interrupting water flows, controls the flooding, it can be potential sites for shelter, nursery, feed ground and refuge for birds (Mitsch and Gosselink, 2000). Therefore, monitoring the vegetation types and

species and their spatial distribution in wetland is a reasonable approach to provide information for local government for better management of wetland resources.

Since getting information from fieldwork is time and money consuming, the task may be partly replaced by new technology. Monitoring wetland by means of satellite remote sensing can be more simple and effective method than field measurements to assess the previous and present wetland status in order to provide information for its management and improvement.

In optical remote sensing, the presence and concentration of leaf pigment of wetland vegetation which response to the light of spectrum, as well as leaf morphology and water content can affect their different appearance on satellite image (Silva et al., 2008). The usual application of optical remote sensing imagery is to map wetland plants in general or classifying it to different populations or vegetation communities. The mapping accuracies rang between 70 to 96% (Everitt et al., 1999; Sawaya et al., 2003; Valta-Hulkkonen et al., 2003; Pasqualini et al., 2005).

However, optical remote sensing has generally failed to identify the similar or some specific vegetation species within the vertical distribution of the canopy, while it has succeeded in identifying the horizontal distribution of vegetation canopies. Moreover, some vegetation species can not be separated due to their similar spectral response (Cohen and Spies, 1992; Woodcock et al., 1994). Additionally, there is a high degree of agreement, considering the radiometric (8 bit), spectral (few, broad bands) and spatial (30 m) limitations of TM-type multispectral images, even better results could be acquired by using more resolving power (Silva, Costa et al., 2008). Besides the instinct limitations of optical satellite imaging systems, another disadvantage is their dependence on the atmospheric conditions while the wetland environments frequently have clouds and smoke obscuring the ground.

By contrast, radar, as an active system, which uses its own energy for illumination the imaged area at different wavelengths, and its energy is capable to penetrate clouds, haze light rain and smoke (Hussin and Shaker, 1996). The use of radar data have been long appreciated as an important tool for studying wetlands. Rather than offering information about biochemical and morphological features, radar data provides information about canopy biophysical characteristics and dielectric properties (a proxy for water content). Since radar sensors are side-looking systems, electromagnetic pulse hits the surface in a subnadir angle, thus most of the radiation is reflected away which does not return to the sensor, when it hits a smooth surface or parallel orientation to the radar look direction. With the increasing of surface roughness and addition of volume components, such as stem/trunk of vegetation, or getting

more perpendicular to the radar look direction, the backscattered radiation increases (Bakker et al., 2004). Therefore, plant characteristics, such as density, distribution, orientation, leaf shape, dielectric constant, height and components of the canopy play an important role in determining the amount of radiation backscattered toward the radar antenna. With this significant relationship between biophysical characteristics and radar backscatter, various researches have shown that radar images can be exploited to study wetland vegetation (Kasischke and BourgeauChavez, 1997; Novo et al., 2002; Kasischke et al., 2003; Moreau and Le Toan, 2003; Costa, 2004).

One of the main shortcomings of satellite radar systems is that most of them have only single band/ polarization configuration, which reduces the accuracy of identification of wetland vegetation (Silva, Costa et al., 2008). Nevertheless, this limitation can be overcome with the combination of different satellite imageries, by means of image fusion.

Fusion of different satellite images aims to integrate different data in order to gain more information than can be extracted from each single sensor data alone. The information provided by optical satellite images shows the multispectral reflectance of the target illuminated by sun light while radar images depend on the characteristics of the illuminated surface target surface. The fusion of these two disparate data contributes to the understanding of the objects observed (Pohl and van Genderen, 1998). Because of this advantage, the number of applications of optical and radar image fusion is increasing, such topographic mapping and map updating (Albertz and Tauch, 1994; Pohl, 1995), land use , agriculture and forestry (Franklin and Blodgett, 1993; Munechika et al., 1993; Hussin and Shaker, 1996; Musa, 1999), flood monitoring (Toyra et al., 2002) as well as ice /snow monitoring (Beaven et al., 1996; Bendjebbour et al., 2001; Bogdanov et al., 2005). The information content is data from various sensor can be different in each other, when joining these sources and if there is low redundancy, the data will permit better mapping and discrimination of vegetation species (Silva, Costa et al., 2008). At usual land cover mapping, accuracies can be increased by 10% after optical-radar fusion (Haack and Bechdol, 2000).

However, the application of merging optical and radar in mapping wetland vegetation is quite less developed. Since the grassland communities in Poyang Lake, China has only been mapped using the Landsat TM imagery (Zeng, 2006) thus radar images can complement optical images using fusion technique in this area.

By assessing and analyzing the integrated data from different sensor we can explore the possibility of applying and define the suitable image fusion technique in order to discriminate

different wetland vegetation communities in the study area, which is the main aim of this research.

1.3. Research Objective

The main objective of this research is to define a suitable fusion technique for combining optical and radar images in order to map the distribution of wetland vegetation communities in Poyang Lake Nature Reserve, China.

The specific objectives are:

1. To map the spatial distribution of the wetland vegetation communities using optical ALOS ANVIR-2 and ENVISAT ASAR Radar satellite images separately.
2. To map the spatial distribution of the wetland vegetation communities using different fusion techniques of combining optical and radar image and compare the map results to single data set maps.
3. To define the most suitable fusion technique of merging optical and radar data for mapping wetland vegetation.

1.4. Research Questions

1. What are the different contents of information between ALOS optical and radar in mapping wetland?
2. How accurate is the information extracted from different fusion techniques of radar and optical data used in this research compare to single data sets?
3. Which fusion technique could separate and mapping the three wetland vegetation communities better for this research in the study area?

1.5. Research Hypothesis

1. The distribution of the main grassland communities can be classified with reasonable accuracy (i.e. 80% or more) from the fused radar and optical remotely sensed images.
2. Classification map of fused image is significantly higher accuracy than the classification of unfused image.

1.6. Outline of the Thesis

The thesis is organized in four chapters follow:

Chapter 1: General introduction of the scientific background of this research is concerned with problem statement and justification of monitoring wetland vegetation. It also consists research objectives, questions and hypothesis.

Chapter 2: Research methods and materials are described in this chapter. It describes the situation of the study area and what kinds of materials are used in this research as well as research methods, which involve data collection, pre-processing and analysis. The procedures of optical and radar data classification, fusion techniques and comparison are explained here.

Chapter 3: Results and discussion: It consists of all the results obtained from the research. They are maps resulted from single data (Optical and Radar) classification. Moreover, the classification of fused data and the comparison of unfused data is presented in this chapter. In addition, results of accuracy assessment of all classification maps are shown. Furthermore, discussion of the results is also presented here.

Chapter 4: This chapter draws conclusion of the results. It also discusses the shortcomings and recommendation of this research to improve the wetland resources management.

2. Materials and methods

2.1. Study area

Poyang Lake national natural reserve area in China which located in the northern part of Jiangxi Province, North Latitude 28°24'- 29°46', East Longitude 115°47'- 116°45' is the largest fresh lake and important international wetland. It is an important storing lake of the main stream of Yangtze River and plays very significant roles in ecological functions, like floodwater storage and biological diversity protection, as well as its economic and social development (Jiang and Piperno, 1999; Guo et al., 2001; Huang, 2006).



Figure 1 Location of Poyang Lake



Figure 2 ALOS image (24 October 2007) for study area (Nature Reserve) using band combinations 4, 2, 1 in RGB

As an important international wetland and famous for plentiful in number of winter waterfowl species, which has a rich biodiversity (102 species of aquatic plants and 122 species of fish), thousands of birds migrating every year from Mongolia, Japan, North Korea and Russia (Kanai 2002) over here to live through the winter time from November to March in the next year (Chen et al., 2007). For the reason to protect rare migratory birds and maintain wetland ecological system, Poyang Natural Reserve was established by the Chinese government in 1983. Natural Reserve, which located in the northwest of Poyang Lake, covers about 300 km². As one of the biggest bird conservation areas in the world, more than 300 birds species among which 50 rare birds have been recorded in the reserve area (Wu and Ji, 2002). The vegetation, especially grass, in that area is the main food for these birds.

The mean water level of Dahuchi Lake in 2005 was 14.08m. The highest water level occurred on September and the lowest came about at January (Guan, 2007). In summer (flood season), water surfaces expand suddenly of every small lake, hundreds of small lakes connecting become one big Poyang Lake. At this time, the landscape in Poyang Lake could be described as an ocean. On the other hand, the water level drops at dry season (December to April in the next year), even the bottomlands become visible which make the landscape of the study area a line at winter (Wu and Ji, 2002).

According to the former research (Guan, 2007) the grassland communities grow along the Lakes have significant seasonal phenology. Their periods of growth are greatly connected with water level which fluctuates with season. There were varieties of natural grass species found in the field which can be categorized into 28 families (Zeng, 2006). The best represented families are the *Graminaceae*, *Cyperaceae*, *Polygonaceae* and *Anthoelinium* while the most normally observed communities are *Carex*, *Miscanthus* and *Cynodon* (see Figure 3). *Carex* community is normally distributed along the lake bank while the other two communities, *Miscanthus* and *Cynodon* are mostly distributed relatively farther from the lake. The terrain here at study area is almost flat ranges from 12 to 18 meters, with less than 6 meter difference between the maximum value and the minimum value. However, within this almost flat area, the vertical distribution pattern of these three vegetation communities could be observed. Close to the lake, *Carex* community grows at a low elevation from 12 to 14 meters. In contrast, the other two grassland communities which distribute further from the lake, grow at a the elevation from 14 to 16 meters (Cai et al., 1997).



Carex

Micanthus

Cynodon

Figure 3 Pictures of the three main vegetation communities

2.2. Research materials

2.2.1. Field data

With the purpose of being scientific and efficient, field work was carried out in study area at the end of October and early November after two months preparation. The aim of the field work was to locate sample plots and collect ground information as training and validating samples for later classification assessment. The total number of wetland vegetation sample was 139. The detail procedure of field survey will be illustrated later in section 2.3.1.

2.2.2. Satellite Imagery and Ancillary Data

The optical image selected for this research was ALOS AVNIR-2 imagery (John and Xiuping, 2006), as this research is supported by the DRAGON II project 5264 and the European Space Agency (ESA). It was acquired on 24th October 2007 which was a clear day without any cloud, thus the quality of that image was very high. The spatial resolution or pixel size of this ALOS image which had four bands (visible blue 0.42 to 0.50 μm , visible green 0.52 to 0.60 μm , visible red 0.61 to 0.69 μm and near infrared 0.76 to 0.89 μm) was 10 m. There were two functions of the ALOS image. The first one was to lead field work which was also took place at the end of October. And the other function was used as the optical data set for vegetation mapping and image fusion.

Multi-temporal C-band ASAR ENVISAT Radar image (Guangmeng et al., 2006) applied in this work, which also provided by DRAGON II project 5264, acquired on 28th October 2008. The wavelength of this image was 5.6 cm. The incidence angle ranged from 25.7° to 31.2°. The image format was alternative polarization precision image (APP) which had two bands VH (Vertical transmission and Horizontal reception) polarisation and VV (Vertical transmission and Vertical reception) polarisation. As an important element in the field of radar remote

sensing, polarisation combination of the obtained backscatter is depending on the polarisation of the transmitted signal power and on the direction (vertical or horizontal) of the scattering elements present in the vegetation. As a general rule, like polarisation (HH and VV) sensing could penetrate vegetation canopy more than cross polarisation HV and VH. Therefore, only VV polarization was used in image fusion procedure for its better performance in present the distribution of vegetation communities. The original pixel size of ENVISAT Radar image was 12.5 m and it was resample into 10 m thus it can be identical to the spatial resolution of ALOS AVNIR-2 image for the fusion purpose.

Topographic map made in 1999 contained information about topography, road network, hill, settlement, water feature and land use. Its scale was 1:10000 and projected in Gauss Kruger. The main function of the topographic map was used as a source for registration all the satellite images to the local projection.

2.3. Research Methods

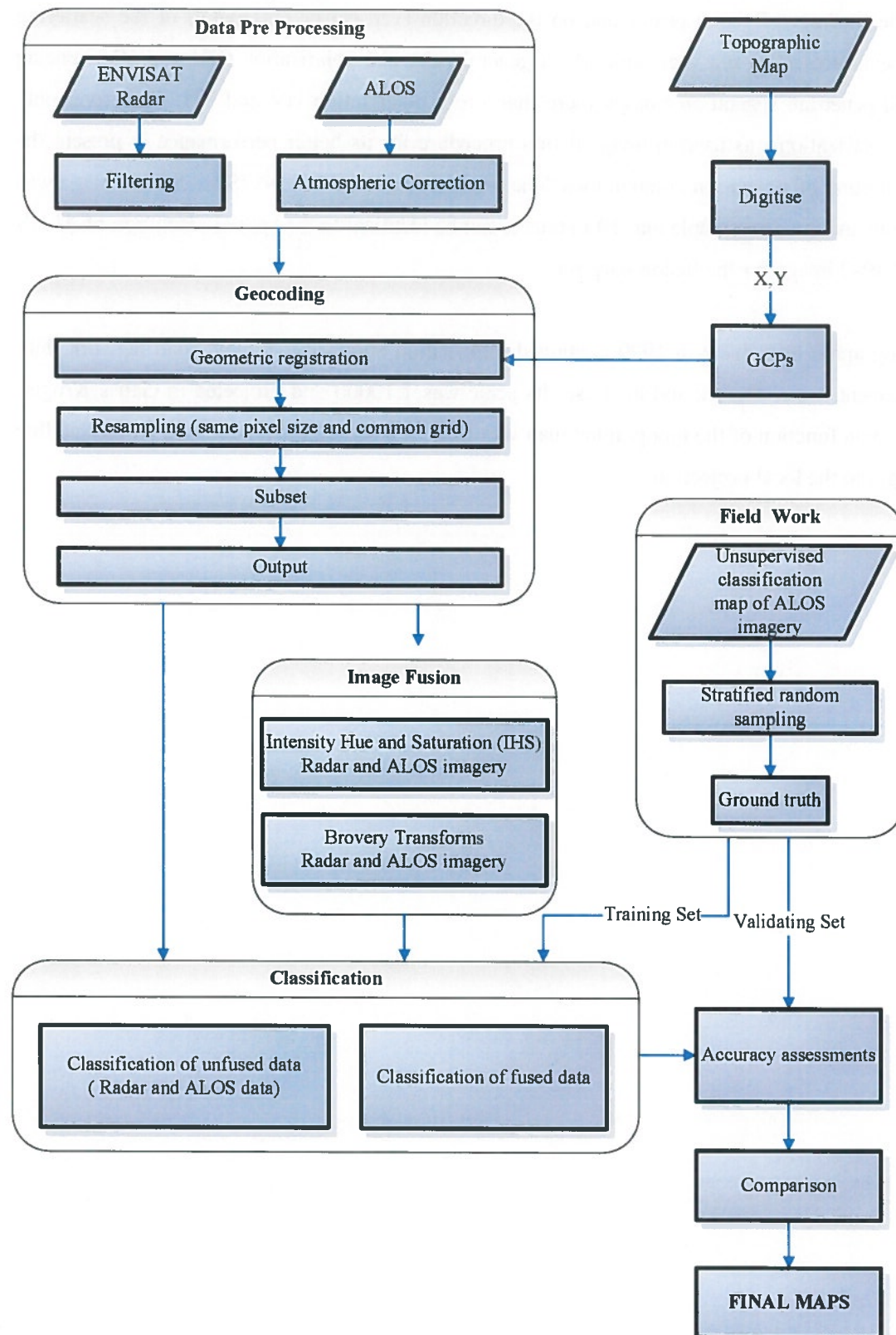


Figure 4 Framework of the research

2.3.1. Field Survey

(This section is written jointly with Xu Chonglin and also appears in her thesis.)

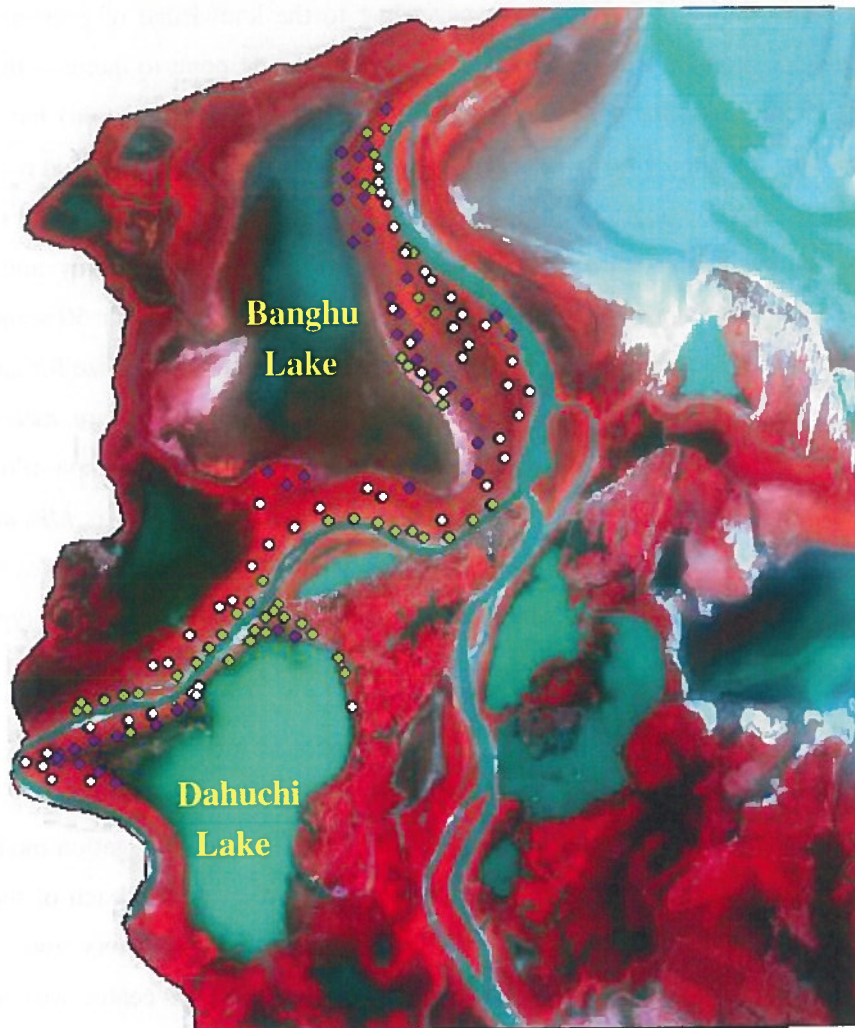


Figure 5 Location of field samples.
(ALOS image on October 24th, 2007)

2.3.1.1. Sample design

Survey for grassland communities was taken before the field data collection. The results were obtained from three parts: an expert in the Institute of Botany in Wuhan Botany Garden, Botanical data (Bruhl et al., 1992; Cai, Ma et al., 1997) and pre-knowledge of the distribution of the grasses and study area (Wu and Ji, 2002; Si, 2006; Zeng, 2006). It was determined that winter sedges are *Carex* communities while summer grasses are *Miscanthus* and *Cynodon* communities.

The Poyang Lake Nature Reserve was heterogeneous and to capture this variation for classification purposes, sampling points were selected based on stratified random sampling

design (Cochran, 1963). Stratification was done using unsupervised classification of the ALOS AVINR-2 Image into 6 land cover types (*Carex* community, *Miscanthus* community, *Cynodon* community, water, hill and sand). It was according to the knowledge of previous research. Clustered random sampling was used at each selected sampling point to increase the sampling size while reducing travelling time. Many researchers (van Gils et al., 2006) have used this sampling strategy in mapping invasive species in South Africa and obtained good results.

Sample size for vegetation survey was according to the required accuracy and had been estimated based on expected standard error. It was recommended that 30 or 50 sampling units are the minimum ones (Van Gils et al., 2006). In the present research, the size for each sample was a circle plot of radius 12.62m which makes an area of 500 square meters. Global Positioning System (GPS) was used to acquire the spatial location of sample plots centers. Data was collected mainly on three dominate grass communities: *Carex*, *Miscanthus* and *Cynodon* and canopy height, soil moisture, density as well as wet biomass. Species dominancy was set at 60% cover and above and used for assigning the main cover type for the classification purpose.

2.3.1.2. Field data collection

The field work was performed during 27th October to 5th November. When we got into the study area (Poyang Lake Natural Reserve) we switched the GPS into navigation mode in order to approach each sample plot. After we reached each plot, we evaluated each of them: if the plot centre was inside one of the three vegetation class, and 30 meters away from the borderline, then this sample was acceptance; otherwise, if the plot centre was inside one vegetation class but less than 30 meters away from the borderline or the plot centre was outside the class but less than 30 meters away from the borderline, the sample was relocated; however if the plot centre was outside any class and more than 30 meters away from the borderline, the sample plot was cancelled. Base on the criteria of acceptance, relocation and cancellation, after ten days of field work, we totally collected vegetation information for 139 points (56 for *Carex*, 50 for *Miscanthus* and 33 for *Cynodon*, see Figure 5).

After evaluation, at each plot we established a circular plot of an area of 500 m² with the radius of 12.62 m (de Gier, 1996). The major vegetation cover which over 60% in one sample plot was identified. The plot information such as average height of the vegetation and biomass was also measured. We chose three 30x30cm square frame randomly in the sampling plot and measure the average height of that vegetation community using a metal measuring tape and cut all parts of the plant above the ground of the three 30x30cm square frame and weigh it to get the fresh or wet biomass (Figure 6).

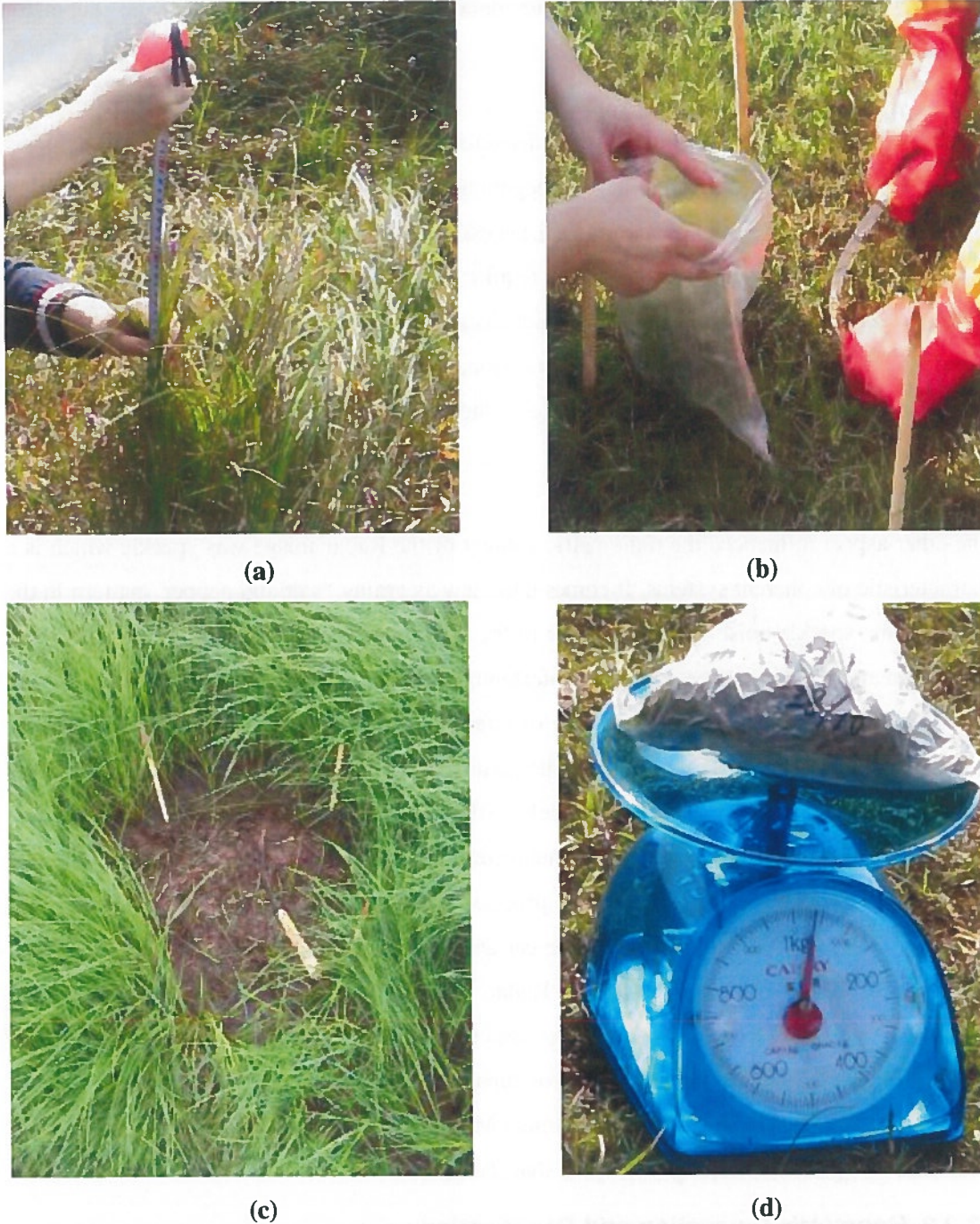


Figure 6 Field work activities (a. measure height of vegetation community; b. cut vegetation above the ground; c. one example of 30x30cm square frame after all the vegetation above the ground; d. weight the fresh biomass of one 30x30cm square frame)

2.3.2. Satellite data preprocessing

2.3.2.1. Radiometric Correction

The two main sources of radiometric distortion in ALOS AVNIR-2 imagery are atmosphere and sensor. Both were already corrected before receiving the data from the source. Owing to

the side-looking viewing geometry, radar data had serious radiometric and geometric distortions.

The ENVISAT ASAR Radar imagery was delivered in 16 bit format. The procedure to convert it into 8 bit format was done in the beginning. Although during the conversion, some information was losing, this step was still necessary (Musa, 1999). Because the conversion would increase the processing speed and require much less storage. Furthermore, in image fusion process, both optical and radar data sets had to be in the same format. ALOS image was in the 8 bit format, for the purpose of image fusion, radar data was rescaled from 16 bit to 8 bit in ERDAS software. Consequently, the pixel value of the new radar imagery varied from 0 to 255.

The other aspect influenced the radiometric content of the Radar image was speckle which is a characteristic of coherent systems. It comes into view as grainy “salt and pepper” pattern in the images. This speckle noise was caused due to the interference of the backscatter signals which came from an area within one pixel. The interference was wave interactions. The return signals became extinguished or amplified because of interference. As a result, it introduced dark and bright pixels to the images. Accordingly, the quality of the images were degraded which made the interpretation of radar imagery difficult. Affecting the radar image’s texture and each individual pixel value, it needed to be minimized in order to perform further analysis like classification and image fusion. Filtering process, which can reduce the speckle noise, was done in ERDAS software. According to the earlier obtained research results (Tzeng and Chen, 2005), three filters were applied on the Radar imagery: Lee-Sigma filter, Frost filter and Gamma MAP filter. Three different window sizes were tested for each filter: 3×3 , 5×5 , and 7×7 . The nine results of the filter-window combinations were shown in Appendix. Based on the visual judgment of the results, the 5×5 Gamma MAP filter was chosen given that it could best smooth the image while keeping the edge’s sharpness.

2.3.2.2. Geometric Correction and Rectification

Geocoding, which is georeferencing with subsequent resampling of the image raster, was the geometric correction approach used in this research. Since it was suitable for the situation when different images need to be combined. There were two steps in this stage: transformation (projection) and resampling. The original image (optical and radar) was rectified with topographic map which was reproject into UTM, N 50 Zone earlier. Therefore that each pixel has a correct geo-location and the same project with the field data which located by GPS. GCPs chose on both master image (topographic map) and slave images (ALOS and ENVISAT Radar) were road crossings, meander, waterways, typical morphological structures and so on

which could easily be identified in the images. In addition to this, the GCPs were distributed in the image dispersedly rather than concentrate at one place in order to minimize the distortion of the original images during georeferencing.

This is followed by resampling which creates square pixel of the projected images (Bakker, Grabmaier et al., 2004). These steps can guarantee the different sensor images to have the same pixel size for the following fusion techniques, which are applied per-pixel. Since the pixel size for ENVISAT Radar image is 12.5m while it is 10m in ALOS optical, considering to preserve the spatial and spectral information of ALOS image and not to lose too much from the original radar information content, a value of 10m of resampling pixel size was chosen.

The choice of the resampling algorithm is made according to the ratio between input and output pixel size and the purpose of the resampled image data. The common methods available of image resampling are nearest neighbour, bilinear interpolation and cubic convolution. The pixels are geometrically changed when performing resample on the imagery (Bakker, Grabmaier et al., 2004). The value of each pixel would be modified or preserved depending on the resampling method applied. Bilinear and cubic convolution resampling methods could lose less spatial information of the original images and produce smoother images than nearest neighbour while resampling. However, the key issue of this research was to do the pixel based classification of each image. The choice on which resampling method to use was made based on the preserving as much as possible the original pixel values. As a result, nearest neighbor algorithms was used in this study to conserve the original DN value. The value of resampled pixel is allotted according to the DN valued of the nearest pixel in the original radar imagery.

Even though both optical and radar images had already registered to the topographic map, it is still necessary to rectify them to each other (Varshney, 1997). It is the key point in image fusion in view of the fact that multisensor image fusion needs all the images are georeferenced to one coordinate system as well as register to each other. Because it was not as easy to identify GCPs in radar image due to its quality compared to ALOS imagery, the procedure of both image georeferenced to topographic map was still necessary.

2.3.2.3. Image subset

The last step of satellite image pre-processing is to subset ALOS and radar images. This procedure was carried out by ERDAS Imagine software. The boundary of the study area was defined according to the area of Natural Reserve of Poyang Lake and made the grassland communities the core issue of the study area.

After all the steps described above of the pre-processing, the final images of ALOS and ENVSAT Radar were ready for further analysis, such as visual interpretation, image fusion and classification and so on.

2.3.3. Image Fusion

Multi-sensor image fusion is the to combine digital data obtained from different sensor with the intention to create a new image through a certain algorithm (Genderen and Pohl, 1994). In order to overcome the problem of the limited availability of up to date optical image from earth resource satellite as well as the cloud free problem, one of the various techniques is image fusion which could merge images from different sensors.

Different techniques can be used to merge remote sensing image (Chavez et al., 1991). In order to find the more suitable fusion technique for mapping wetland vegetation, two different fusion techniques were applied in this research. The first one was Intensity, Hue and Saturation (IHS) and the other one was Brovey Transform.

For IHS image fusion, the data set were fused by means of replacement of the combination intensity of the optical bands, by the intensity of radar image (Hussin and Shaker, 1996). The IHS transformation which separated spatial (I) and spectral (H, S) information from a standard RGB image was considered as a standard procedure in image analysis effectively (Pohl and van Genderen, 1998). The transformation will be applied to ALOS single band 4, 2, 1 and Radar image through map calculation module in ILWIS software. The equations used in this research was developed by Hussin and Shaker (1996) shown as below. In the equation, Image 1, Image 2, and Image 3 were substituted by ALOS band 4, 2, 1.

$$\begin{aligned} \text{Red Image} &= (\text{Image 1}^{2/3}) - (\text{Image 2}^{1/3}) - (\text{Image 3}^{1/3}) + (\text{Radar Image} * 1/\sqrt{3}) \\ \text{Green Image} &= (\text{Image 2}^{2/3}) - (\text{Image 1}^{1/3}) - (\text{Image 3}^{1/3}) + (\text{Radar Image} * 1/\sqrt{3}) \\ \text{Blue Image} &= (\text{Image 3}^{2/3}) - (\text{Image 1}^{1/3}) - (\text{Image 2}^{1/3}) + (\text{Radar Image} * 1/\sqrt{3}) \end{aligned}$$

Equation 1 IHS Transformation (Hussin and Shaker, 1996), Image 1, 2 and 3 substituted by optical ALOS 4, 2, 1

The other procedure known as Brovey Transformation is based on the normalization of sun illumination in the optical images and the subsequent multiplication with radar image (Hussin

and Shaker, 1996). The transform was developed to visually increase contrast in the low and high ends of an image histogram. It is a simple way to fuse multisensor image data. Followed the same methods as IHS, the equations were given below:

$$\begin{aligned} \text{Red Image} &= \text{Image 1} / (\text{Image 3} + \text{Image 2} + \text{Image 1}) * \text{Radar Image} \\ \text{Green Image} &= \text{Image 2} / (\text{Image 3} + \text{Image 2} + \text{Image 1}) * \text{Radar Image} \\ \text{Blue Image} &= \text{Image 3} / (\text{Image 3} + \text{Image 2} + \text{Image 1}) * \text{Radar Image} \end{aligned}$$

Equation 2 Brovey Transformation (Hussin and Shaker, 1996), Image 1, 2 and 3 substituted by ALOS 4, 2, 1

2.3.4. Image Classification

Classification of remotely sensed data assigns every pixel in the image to one class which has a specific spectral response on the ground (Lillesand and Kiefer, 1994). The supervised classification was performed by Maximum Likelihood Classifier. It was the classifier calculated the probability of a given pixel belongs to which specific class. The reason for selecting this algorithm was that it had been generally proven to be the one can achieve the best result for classification of remotely sensed data (Michelson et al., 2000). Besides three vegetation communities, water and sand will be classified in all unfused and fused images while hill was masked in all the images.

Maximum Likelihood classification was performed in ERDAS software which included three main steps: selecting training samples, generating the spectral signatures of training samples and classification of the area based on the signature generated from the training samples.

2.3.5. Accuracy Assessment

The accuracy assessment methods used in this research were error matrix (also called confusion matrix) and Kappa statistic. Error matrix was one of the most common ways to assess the accuracy of the classification results. It was an efficient tool which provides two groups of classes reporting the accuracy of a final map (Stehman, 1997). The columns represented the reference data (ground truth) while rows represented the classification results. The accuracy for a specified class was given by the errors of inclusion (commission errors) and exclusion (omission error) of reference data units into the class. The producer's accuracy was the ratio between the number of correctly classified sampling units of one class and the total number of the reference sampling units for this class, while user's accuracy was given by dividing the total number of correctly classified units by the number of units misclassified to this class (Congalton, 2001).

Kappa statistic signified how each class differed from random classification of reference data after it measured the magnitude differences in accuracy (Lillesand and Kiefer, 1994). Being a currently popular multi-variate statistical technique for accuracy assessment, Kappa statistic could also be used to test the classification accuracy based on error matrix. Since Kappa analysis could take into account the whole error matrix rather than only producers or overall accuracy which may lead biased toward one of the categories (Tung and Ledrew, 1988).

2.3.6. Testing for a Significant Difference between Images

The comparisons among the accuracy of classification maps were base on single accuracy parameter such as producers, users and overall accuracies. However, the aim of this research is to compare the error matrix from the classification results of two remotely sensed data sets. As a consequence, the appropriate parameter, which could signify summary measure of the error matrix, was used. The value of kappa statistics and their large sample variance were used to compare the performance of classification results of both unfused data sets and fused data sets. The test of significance known as the comparison between two erro matrices significantly different or not was introduced here. The kappa statistical value and their associated variance for the two images were tested by evaluationg the normal curve deviate statistic (Z) for $\alpha = 0.05$ (Cohen, 1960; Bishop et al., 1975; Ma and Redmond, 1995).

3. Results and Discussion

3.1. Single Images

Two image data sets were applied in this study. The optical data was ALOS AVNIR-2 image while the radar data was ENVISAT ASAR Radar. These two data sets were interpreted individually in order to get a better understanding of further image classification and image fusion.

3.1.1. ALOS Optical Image

The color composite ALOS imagery is shown in Figure 7, with band 4 in red, 2 in green and 3 in blue. In general, the vegetation communities (*Carex*, *Miscanthus* and *Cynodon*) grown around the two big lakes and along the river appear in red. However, the saturation of the red color is different in belt shape around the lakes, especially the northern lake named Banghu Lake. The water represents a blue-green tone. Since the turbidity of each lake or river was different so was the depth, the color of some lakes are darker than the other ones. The unique white color in the northeast part of the study area is sand. The hill close to the southwest lake (Dahuchi Lake) is also red, although the red tone is slightly different with vegetation communities, it is still a little confusion between these two classes.

3.1.2. ENVISAT Radar Image

Figure 8 shows the single band of ENVISAT ASAR Radar imagery. The water areas are very obvious in the black colour without any discrimination of turbidity or depth of the water as compared to ALOS optical image. However, due to the reflectance principle of radar system, some part of the sand area is as flat as water area, which also appears black as the water appears. This is because these two surfaces are smooth to the radar energy, thus the radar energy would bounce away from the antenna and consequently it will appear dark. So it could be more difficult to differentiate water and sand in radar imagery than in ALOS optical imagery.

The ENVISAT Radar imagery has short wavelength (C band, 5.6 cm) and vertical (VV) polarization induce that the radar signal is dominantly scattered by hill. This is the reason for the lighter tone of hill than vegetation communities. And this also leads to the different gray scale of the vegetation communities in belt shape next to Banghu Lake. Moreover, since the vegetation community grown along the lake was much shorter in height than the one developed



Figure 7 ALOS optical image (band 4, 2, 1 assigned to red, green and blue) of the study area

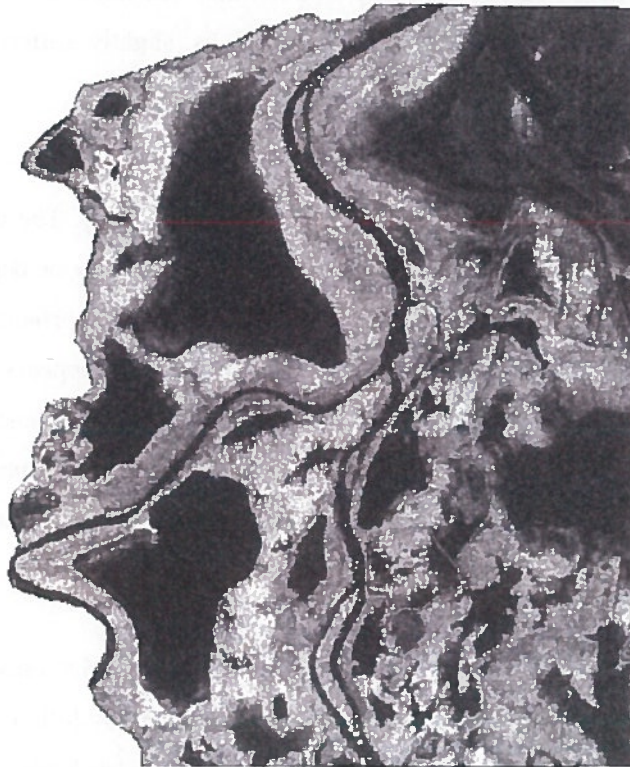


Figure 8 ENVISAT ASAR Radar (VV-polarized) of the study area

along the river, the radar signal scattered away was less in the short one which appears lighter tone in the image.

3.2. Fused Images

Considering the areas shown clearly in ALOS imagery and radar imagery respectively were different, in the ALOS image water and sand could be differentiated easily but vegetation communities were similar with hill while it was the opposite situation in radar imagery, we could expect fused images would perform better in visual interpretation by combining both images together.

3.2.1. Brovey Transformation

Figure 9 illustrates the effects of Brovey Transformation technique of fusing ALOS optical data set and ENVISAT Radar data set. The radiometric content in the original ALOS image was affected, while the intensity in the original bands was substituted after being sum-normalized. Accordingly, the saturation value of the image was maintained with only the intensity substitution (Kuplich et al., 2000). The spectral content of the ALOS imagery was preserved with the introduction of the texture content from radar imagery (Pohl and van Genderen, 1998).



Figure 9 Result of Brovey Transformation technique applied to ALOS and radar images

In the result image of Brovey Transformation of ALOS and radar imagery, the water-land boundaries were defined very well, especially compare to ALOS imagery. Since the radar

signal was all reflected away when it reached the surface of water without affected by the content of the water, such as sediment concentration and depth, all the water area shown in a dark tone close to black in the image. This was the character generated from the radar imagery, which helped further image interpretation by supervised classification. Geometrically, water is a smooth surface to the radar energy. As a result most of the incident energy on water will reflect away (specular reflection) and hardly any radar energy will return to the antenna. Therefore, a surface like water or even smooth soil or sand would show on radar image in dark tone (Figure 10). However any rough surface to the radar energy will have a diffuse reflection. This means that the energy will be scattered in all direction. Consequently considerable part of the energy will return to the radar antenna. Therefore, such a rough surface will show in light gray tone depending on the degree of roughness.

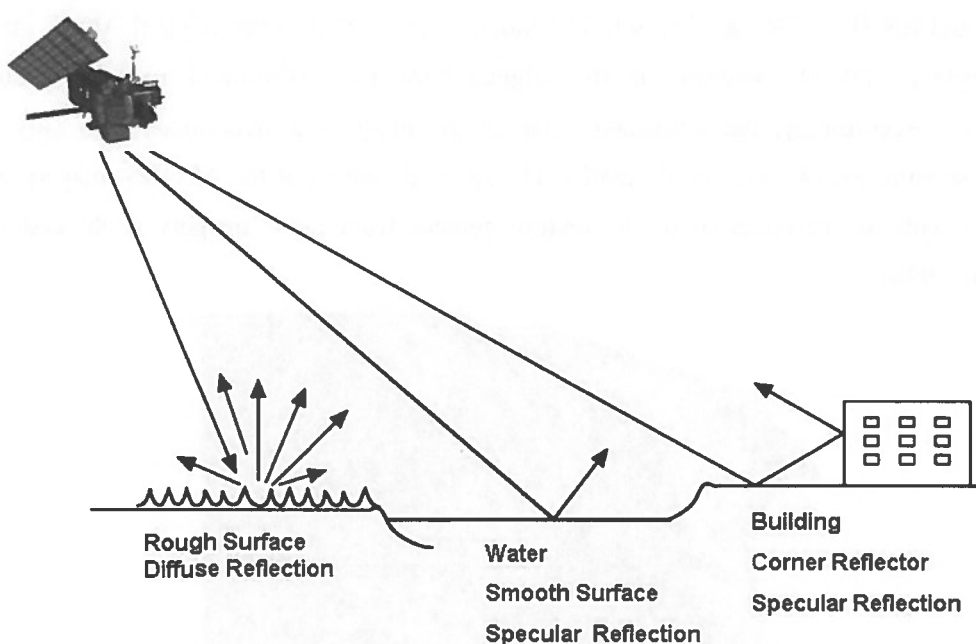


Figure 10 Radar returns as a function of geometric properties of object (Lillesand and Kiefer, 1994)

Considering the above statement, using radar imagery alone would not be possible to differentiate between water and sand. However using Brovey Transformation by combining optical, which clearly differentiate water from sand, and radar we could differentiate sand from water bodies. The surface of the sand area was as flat as water which caused the specular reflection of radar signal, few signal returned back to the radar antenna, which also show a dark tone in sand cover area. Nevertheless, the dark tone for sand area was close to dark green which could be distinguished easily from the black water area. The dark green is the contribution of ALOS optical image which had a high spectral resolution. The above explanation shows that radar and optical images complement each other in contribution of

information that can be extracted and help the classification or mapping resources. Thus Brovey Transformation generated the good quality aspects from both optical data set and radar data set.

3.2.2. Intensity Hue and Saturation (IHS)

The other fusion result from Intensity Hue and Saturation Transformation is shown in Figure 11.

During IHS Transformation, the saturation was affected by the intensity substitution. Image fusion processing was an exchange between spectral information and spatial information. Spectral information changed from low spatial to high spectral resolution sensor while spatial



Figure 11 Result of Intensity Hue and Saturation (IHS) technique applied to ALOS and radar images

structure changed from high spatial to low spectral resolution sensor (Cracknell, 1992). The IHS Transformation proffered a controlled visual illustration of fused data. Being used readily exclusive and quantifiable color attributes, informative features which were presented through IHS could be distinctly observed (Harris et al., 1990).

The speckle noise was preserved from the radar data in the fused result and spectral content of the imagery shows similarities with Brovey Transformation (Pohl and van Genderen, 1998). By comparing both fused imagery, the IHS result looks noisier, on the other hand, the distinction

between each class, especially between vegetation communities which grown around the lakes and grown along the river, is much more clear in IHS result which was an impression of high sharpness.

The IHS fused result also shows good quality generated from both optical and radar data set. For water covered areas, the image illustrates them as dark green. And the unique purple color in the northeast part of the study area represents sand area. As a result, water and sand cover could be told apart effortlessly. What's more, hill in the middle shows as extremely lighter tone close to white while the vegetation communities around the lakes are green and red in different saturations.

Nevertheless, the IHS imagery reduced the spatial detail compared to the original optical data (Pohl and van Genderen, 1998), so it looks less clear in general comparing to ALOS image. After visual interpretation of both single data set (ALOS and ENVISAT RASAR) and fused result (Brovey and IHS transformation), it can be concluded that the latter performed better in visually differentiating most of classes than single data set alone.

3.3. Classification Results

The supervised classification is founded on each pixel of the images. Maximum Likelihood Classifier was used for all the images. The results of all the classification images are illustrated in colored thematic maps. Qualitative and quantitative evaluation was made for each classification result.

3.3.1. Training and Validating Samples

Field data which contain 139 sample plots of the vegetation communities were divided into two parts: almost 50% (70) of the sampling plots were selected randomly as training sample in supervised classification, the other half (69) were chosen as the validating sample. Hill was then overlaid to the classification maps as it was masked in the beginning. Table 1 demonstrates the sample design for training and validating sample plot.

Table 1 Training and validating sample for maximum likelihood classification

Class	Field sample	Training sample	Validating sample
<i>Carex</i>	56	28	28
<i>Miscanthus</i>	50	25	25
<i>Cynodon</i>	33	17	16
Water	60	30	30
Sand	20	10	10
Hill	0	0	15

Total	219	110	124
-------	-----	-----	-----

3.3.2. Single image mapping

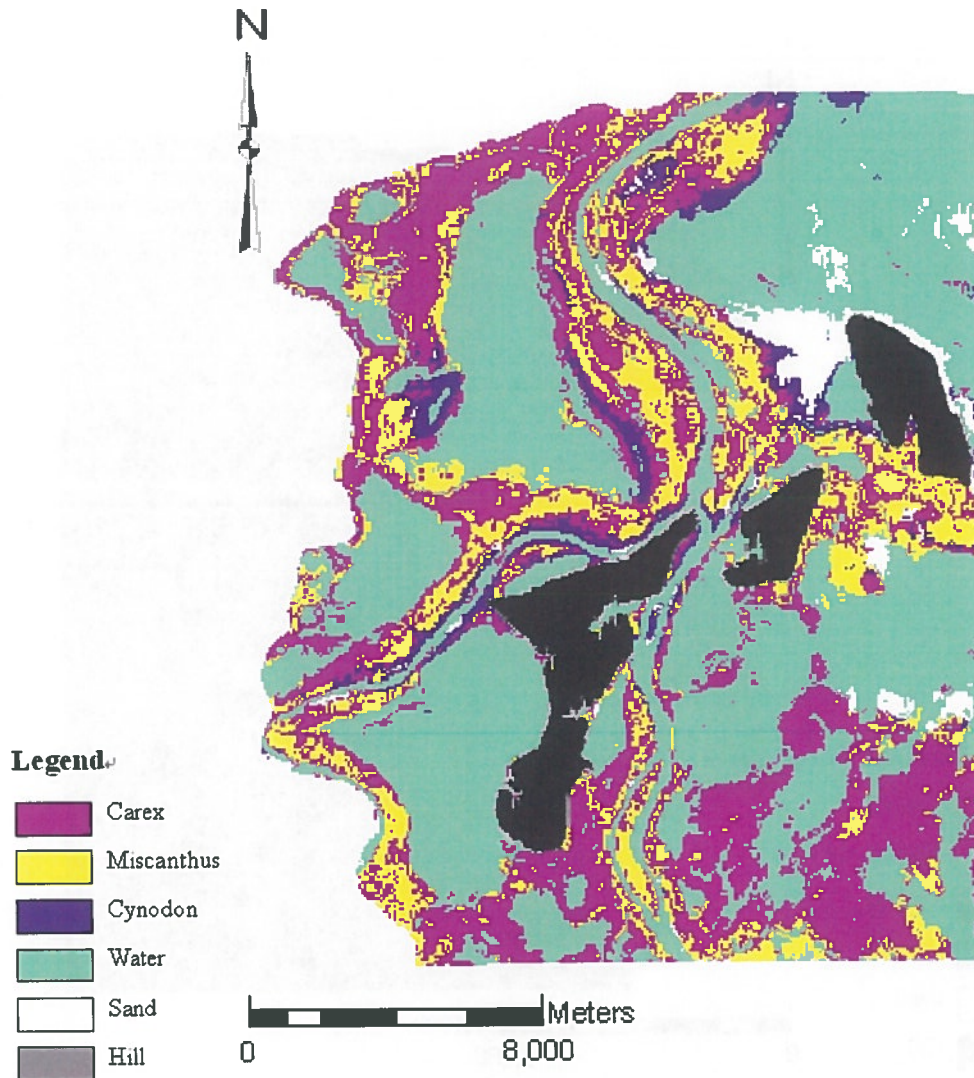


Figure 12 Classified image of ALOS

The ALOS imagery classification map is shown in Figure 12. In general, the colored classification map of the study area demonstrates water in blue color, sand for white color, hill for grey color. The three grassland communities (*Carex*, *Miscanthus* and *Cynodon*) are pink, yellow and purple respectively. Partly of the *Miscanthus* class and the *Carex* class around Banghu Lake were misclassified with each other. Normally, most part of *Miscanthus* are grown further from the lake comparing to *Carex* (Cai et al. 1997). However, from the classification result of ALOS image only, it is hard to tell which one of them was further from Banghu Lake. The *Cynodon* class is illustrated well in the imagery; most of them grow along the river (Zhang et al., 1998).

The sand class also showed well which located in the northeast part of the study area. Conversely, the water class was misclassified often in the imagery. In Banghu Lake, it is very clear to see that some parts of the water bodies were classified into *Carex* and *Miscanthus*. The

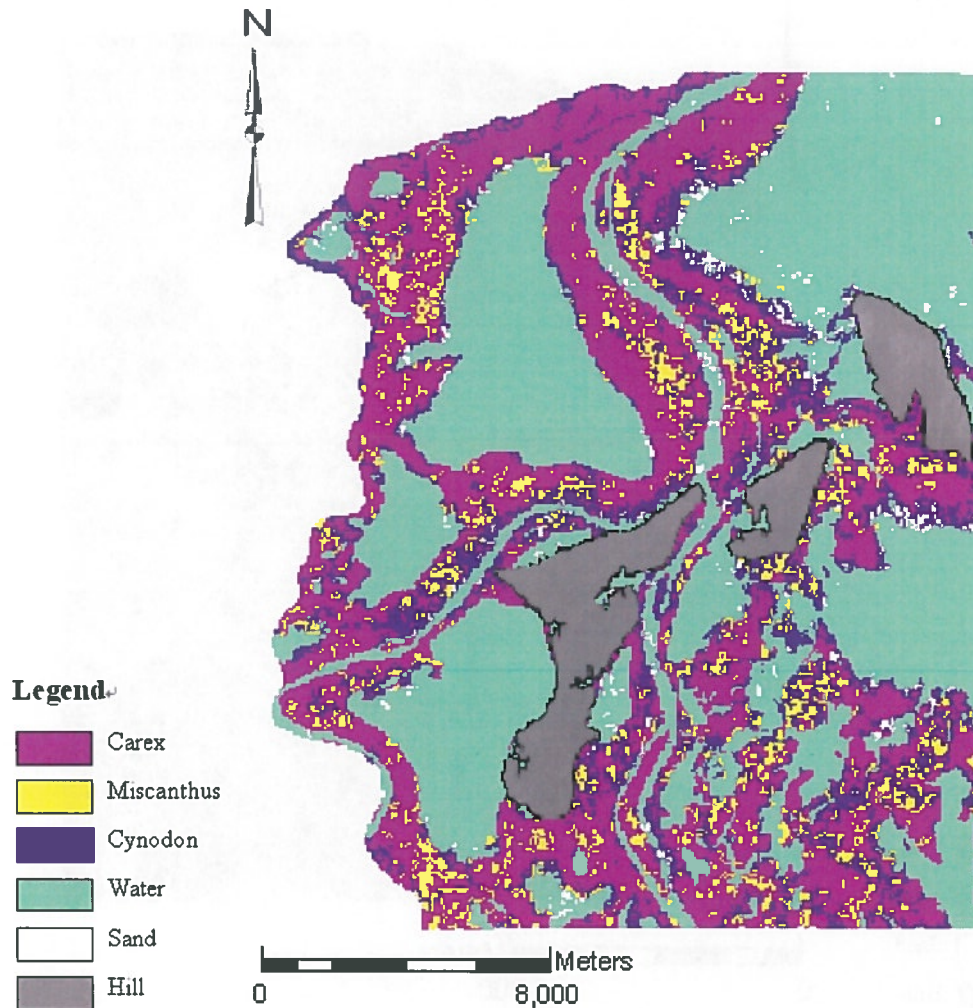


Figure 13 Classification map of the ENVISAT Radar image

misclassification also happened in the northeast lake where some parts of the water were classified as sand, since the turbidity of that lake was very high, the spectral reflectance between turbidity water and sand in optical imagery are close.

Figure 13 is the classification mapping of ENVISAT Radar image. The color for each class is the same with ALOS classification map. Speckle noise of the radar image has made the process of classification difficult. Moreover, this character also led to the frequent misclassification in different class.

Misclassification happened all over the three vegetation communities. Most of area was classified into *Carex* class. Only few part of *Cynodon* was corrected shown along the river. Additionally, sand could barely tell from the classification result of radar. Most of the sand areas were misclassified into water class, since both surfaces are smooth with which the radar energy would specularly reflected away from the radar antenna. However, the water bodies in this map were defined clearly.

3.3.3. Fused image mapping

The results of the first fused image mapping are shown in Figure 14 (Brovey Transformation) and Figure 15 (IHS Transformation).

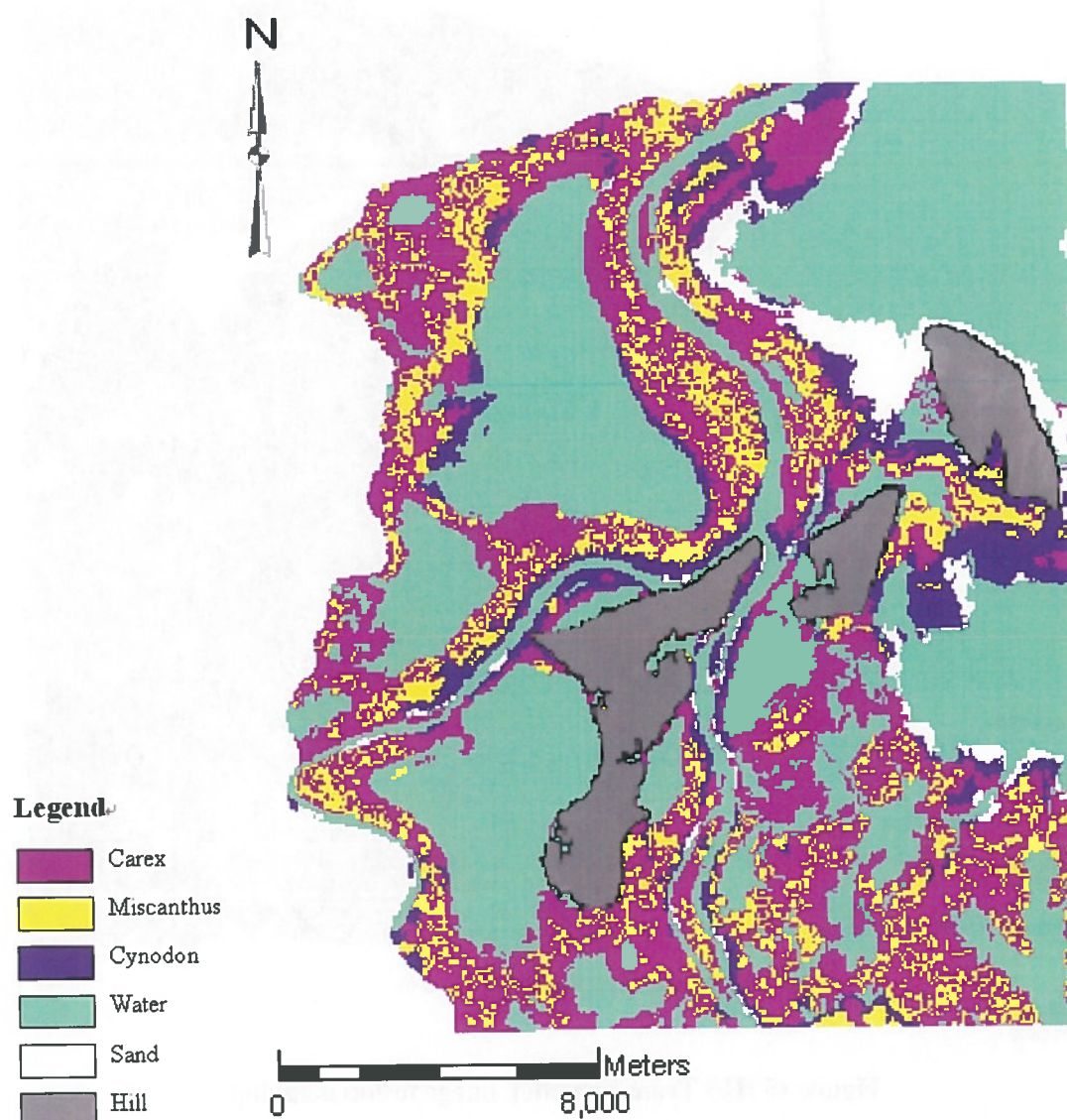


Figure 14 Brovey Transformation image fusion mapping

As what we expected, the fused images generated both good qualities from the optical data set and radar data set, the results of their classification maps had performed better than either ALOS imagery or radar imagery only.

The boundary of water bodies were well defined in both Brovey and IHS fused classification map. Without any misclassification with three vegetation communities, the water classes in two images were also separated with sand classes completely. Sand classes shown in white color are very clear in both images.

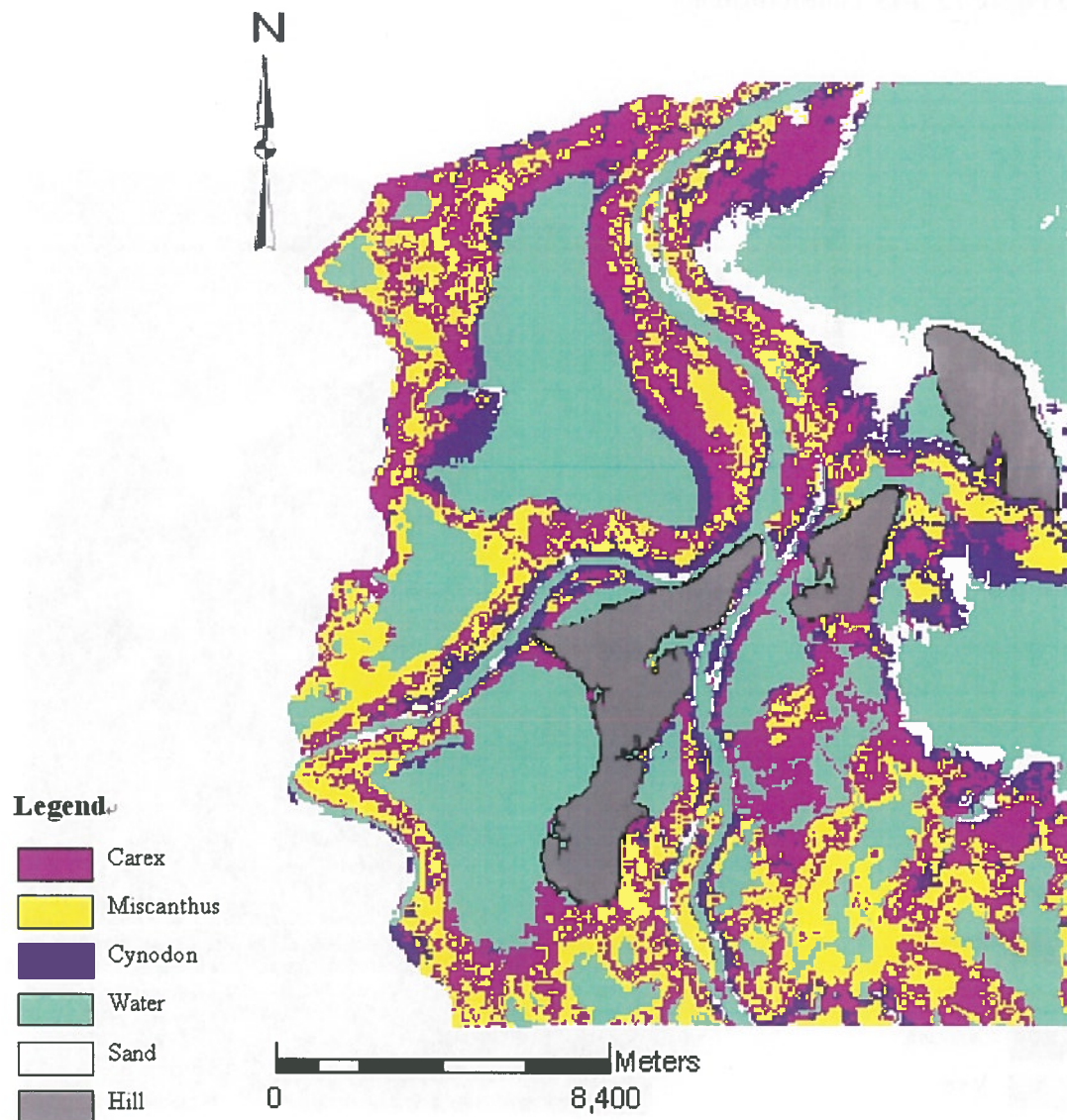


Figure 15 IHS Transformation image fusion mapping

For the three vegetation communities, we could see from the images, *Carex* was the one closest to the lake, followed by *Miscanthus*. *Cynodon* usually grew along the river. However, comparing between the two fused image maps, it is obvious to see the three vegetation

communities are presented in the belt shape in the IHS fused map. In Brovey fused classification map, we can only observe the order of closeness of three vegetation class to the lakes. *Miscanthus* class in this imagery is much scatter than in the IHS classification map and it could barely forms the belt shape as it supposed to. On the other hand, this vegetation class performs much better in the IHS classification map, it is in the belt shape which further from the lakes than *Carex* class.

3.3.4. Classification Accuracy Assessment and Comparison

After the classification of each image and visual comparison, it is necessary to assess the quantitative aspect of the accuracy of the results obtained. By assessing the accuracy of these classification results, we can analyze the results quantitatively by comparing conformity of the classification map and the ground reference data. This was reflected by error matrix which offered user's, producer's and overall accuracies. And the performance of each classification results could also be compared kappa analysis.

Table 2 Error matrix for supervised classification of ALOS optical imagery

Classified Data	Reference Data						Total
	Carex	Miscanthus	Cynodon	Water	Sand	Hill	
Carex	25	2	2	2	0	0	31
Miscanthus	2	21	2	1	0	0	26
Cynodon	1	2	12	0	0	0	15
Water	0	0	0	27	0	0	27
Sand	0	0	0	0	10	0	10
Hill	0	0	0	0	0	15	15
Total	28	25	16	30	10	15	124

Table 3 Accuracy assessment for supervised classification of ALOS optical imagery

Class Name	Reference Totals	Classified Totals	Number Correct	Producers Accuracy	Users Accuracy
Carex	28	31	25	89.29%	80.65%
Miscanthus	25	26	21	84.00%	80.77%
Cynodon	16	15	12	75.00%	80.00%
Water	30	27	27	90.00%	100.00%
Sand	10	10	10	100.00%	100.00%
Hill	15	15	15	100.00%	100.00%
Overall Classification Accuracy = 88.71%					
Overall Kappa Statistics = 0.8875					

From Table 2 and Table 3 which show the error matrix and accuracy assessment of the classification mapping result of ALOS imagery, we could see that sand class was inclusive classified correctly. All of the validating samples of sand fell into the right class (Producer's accuracy is 100%) and none of the validating samples from the other class were misclassified into sand class (User's accuracy is 100%). Within the three grassland community classes, *Carex* had the highest accuracy while *Cynodon* had the lowest.

Table 4 Error matrix for supervised classification of ENVISAT Radar imagery

Classified Data	Reference Data						Total
	Carex	Miscanthus	Cynodon	Water	Sand	Hill	
Carex	21	8	5	0	0	0	34
Miscanthus	4	14	1	0	0	0	19
Cynodon	3	3	10	0	0	0	16
Water	0	0	0	30	7	0	37
Sand	0	0	0	0	3	0	3
Hill	0	0	0	0	0	15	15
Total	28	25	16	30	10	15	124

Table 5 Accuracy assessment for supervised classification of ENVISAT Radar imagery

Class Name	Reference Totals	Classified Totals	Number Correct	Producers Accuracy	Users Accuracy
Carex	28	34	21	75.00%	61.76%
Miscanthus	25	19	14	56.00%	73.68%
Cynodon	16	16	10	62.50%	62.50%
Water	30	37	30	100%	81.08%
Sand	10	3	3	30%	100%
Hill	15	15	15	100%	100%
Overall Classification Accuracy = 75.00%					
Overall Kappa Statistics = 0.6805					

Table 4 and Table 5 demonstrate the quantitative result of the accuracy obtained from radar imagery classification. As the same with ALOS classification result, *Carex* had the highest accuracy from the three vegetation classes. However, instead of *Cynodon*, *Miscanthus* community was the lowest one. Some parts of the *Miscanthus* were misclassified into *Carex*. This happened because in the field, early growing stage *Miscanthus* was similar with *Carex* in some aspects such as height and density. Thus it was hard to differentiate them in radar imagery. Nevertheless, the color of *Miscanthus* was gold while it was green for *Carex*, there were differences between them in optical imagery due to different spectral reflectance.

The accuracy of sand was very low in radar classification map, while the accuracy was 100% for water.

Table 6 Error matrix for supervised classification of fused image using Brovey Transformation technique

Classified Data	Reference Data						Total
	Carex	Miscanthus	Cynodon	Water	Sand	Hill	
Carex	26	4	1	0	0	0	31
Miscanthus	2	20	0	0	0	0	22
Cynodon	0	1	15	0	0	0	16
Water	0	0	0	30	0	0	30
Sand	0	0	0	0	10	0	10
Hill	0	0	0	0	0	15	15
Total	28	25	16	30	10	15	124

Table 7 Accuracy assessment for supervised classification of fused image using Brovey Transformation technique

Class Name	Reference Totals	Classified Totals	Number Correct	Producers Accuracy	Users Accuracy
Carex	28	31	26	92.88%	83.87%
Miscanthus	25	22	20	80.00%	90.91%
Cynodon	16	16	15	93.75%	93.75%
Water	30	30	30	100%	100%
Sand	10	10	10	100%	100%
Hill	15	15	15	100%	100%
Overall Classification Accuracy = 98.58%					
Overall Kappa Statistics = 0.943					

Comparing to single image classification maps, the result from Brovey Transformation map was much better (Table 6 and 7). The accuracy for each vegetation community class was higher than single imagery. Especially for *Cynodon* class, the producer's accuracy raised from 75% (ALOS) and 62.5% (radar) to 93.75% in Brovey fused map. The reason for this is that information got from single imagery was complementary to each other during fusion procedure. This kind of vegetation community was very short, only 10 cm below; and its densities were far less than either *Carex* or *Miscanthus* community. Spectral reflectance generated from ALOS image combine with information obtained from radar data (height and density) formulated the high accuracy in the fused image for *Cynodon* community.

Both water and sand had the classification accuracy of 100%. This also happened because complementary aspects of information obtained from single ALOS optical and ENVISAT ASAR Radar image.

Table 8 Error matrix for supervised classification of fused image using IHS Transformation technique

Classified Data	Reference Data						Total
	Carex	Miscanthus	Cynodon	Water	Sand	Hill	
Carex	26	3	1	0	0	0	30
Miscanthus	1	22	1	0	0	0	24
Cynodon	1	0	14	0	0	0	15
Water	0	0	0	30	0	0	30
Sand	0	0	0	0	10	0	10
Hill	0	0	0	0	0	15	15
Total	28	25	16	30	10	15	124

Table 9 Accuracy assessment for supervised classification of fused image using IHS Transformation technique

Class Name	Reference Totals	Classified Totals	Number Correct	Producer Accuracy	User Accuracy
Carex	28	30	26	92.88%	86.67%
Miscanthus	25	24	22	88.00%	91.67%
Cynodon	16	15	14	87.50%	93.33%
Water	30	30	30	100%	100%
Sand	10	10	10	100%	100%
Hill	15	15	15	100%	100%
Overall Classification Accuracy = 94.38%					
Overall Kappa Statistics = 0.9250					

As in the results of Brovey Transformation, the benefit for fused image classification could also be observed from IHS Transformation map accuracy results (Table 8 and 9). Water and sand were totally corrected classified (100%). The accuracy of *Miscanthus* was raised from 80% to 88% comparing to Brovey result. Although the accuracy of *Cynodon* decreased (from 93.75% to 87.50%) it was mainly because of the small number of validation sample of *Cynodon* (16). 15 of them were correct in the Brovey result and it was 14 in the IHS result.

In order to make it clear and easier to compare each accuracy result, figure 16 provides the comparison between each classification of overall accuracy and Kappa statistics.

From Figure 16, it is very easy to find out the fact that, fused images (Brovey and IHS) had higher overall accuracy and Kappa statistic than single images (ALOS optical and ENVISAT Radar). The accuracies were even lower in radar imagery than ALOS data. The explanation for this was that only one band (VV) of radar image was applied in this research while ALOS

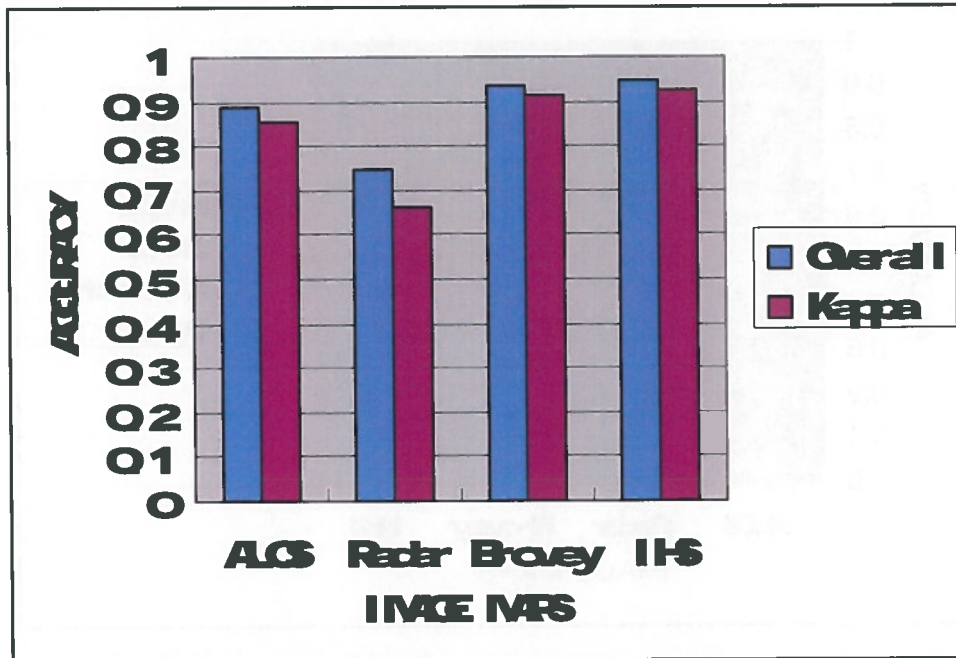


Figure 16 Comparison of single images and transformation images by overall accuracy and Kappa statistic

imagery had four band. Another reason is the speckle noise in radar image made the process of classification radar data rather difficult because speckle noise would increase the variability which consequently increases the covariance of the classes which resulted in overlap between the classes and reduce the accuracy. Although the speckle was minimized by the Gamma MAP filter, it was still the basis of the poor result of classification map of radar data.

Between two fusion techniques, the IHS Transformation had slightly better accuracy results than Brovey Transformation. We could conclude from this that, IHS performance of separability of wetland vegetation was higher than Brovey transformation.

Wetland vegetation community mapping is the key issue of this research. Accuracy information for the three vegetation communities was extracted from each classification accuracy results. Figure 17 and 18 shows the producers/users accuracy and Kappa statistic of three vegetation communities with both unfused and fused images in curve and bars. The bar represents the Kappa statistic of each map; the pink, yellow and purple curves illustrate the accuracy assignment in each image map of *Carex*, *Miscanthus* and *Cynodon* respectively. Since

considering only one of the producers or users accuracy may lead to biased toward the categories (Tung and Ledrew, 1988), Kappa statistic used in the graphs to balance the assessment. Still, the trend of each curve is the same with Kappa analysis: lower in radar imagery, higher in fused images with ALOS optical image in the middle.

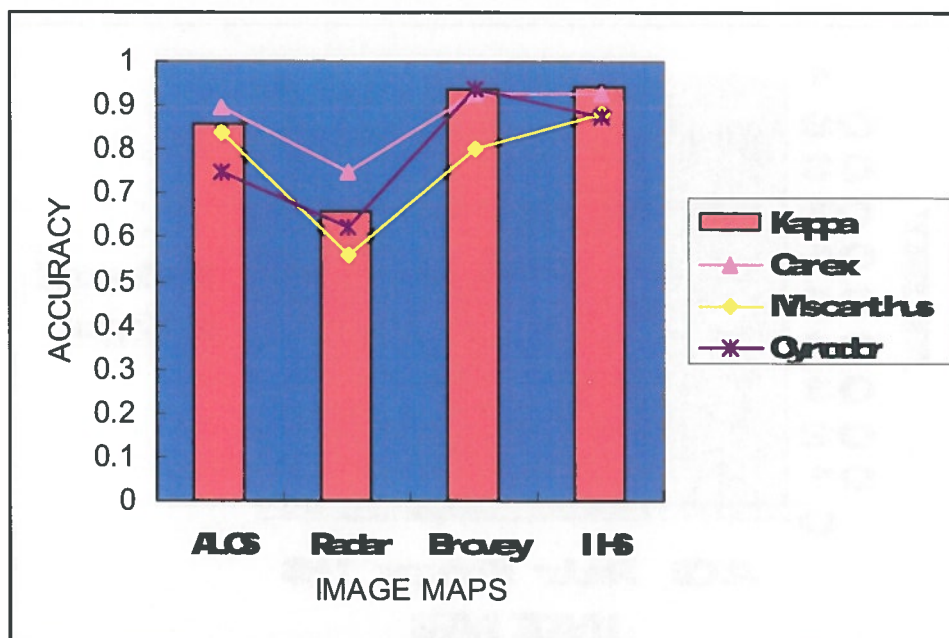


Figure 17 Producers accuracy and Kappa statistic of three vegetation communities with both unfused and fused images

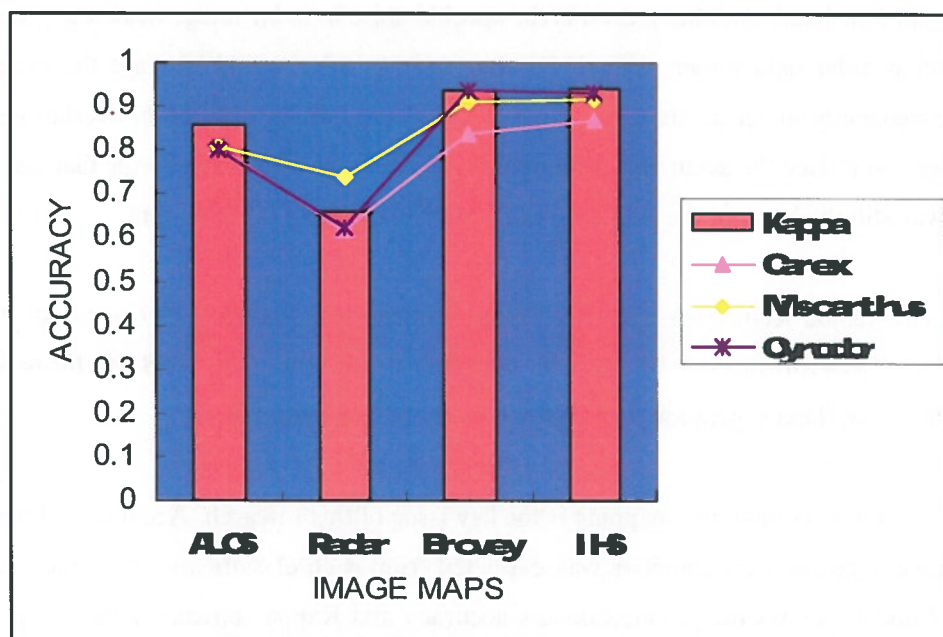


Figure 18 Users accuracy and Kappa statistic of three vegetation communities with both unfused and fused images

From these two figures, it was easily to get a better understanding of the classification benefit gained from image fusion process. The fused images had higher accuracy of each grassland vegetation community than any of the unfused data. The higher Kappa values in two fused classification map were raised comprehensively from the increasing of every vegetation class rather than the enhancement only one or two vegetation communities. In another word, the fusion technique used in this research could separate these three classes better than the original single image and resulted in higher accuracies in the classification map.

Table 10 Accuracy comparison between three vegetation communities with single image (ALOS and radar) classification map and fused image (Brovey and IHS) classification map

Class Name	ALOS		Radar		Brovey		IHS	
	Prod%	User%	Prod%	User%	Prod%	User%	Prod%	User%
<i>Carex</i>	88.29	80.66	75.00	61.76	92.86	88.87	92.86	86.67
<i>Miscanthus</i>	84.00	80.77	56.00	73.68	80.00	90.91	88.00	91.67
<i>Cynodon</i>	75.00	80.00	62.50	62.50	93.75	93.75	87.50	93.33
Overall accuracy	88.71%		75.00%		93.58%		94.38%	
Kappa statistic	0.8875		0.6805		0.9143		0.9250	

As we could see from Table 10, which illustrates the extracted accuracy information of three vegetation classes, the bold numbers are the highest one in one category. The highest producers accuracy for *Carex* was in both Brovey image and IHS imagery (92.86%) while the highest users accuracy 86.67% of this class was in IHS image. The top values of both producers (88.00%) and users (91.67%) accuracy of *Miscanthus* were in the IHS Transformation fused image. The highest accuracies of *Cynodon* 93.75% (producers and users) were in the Brovey image; still, the values in IHS (87.00% and 93.33%) were very close to the highest ones. In general, IHS transformation offered slightly superior results in this research which had the highest overall accuracy (94.35%) and Kappa statistic (0.925).

3.3.5. Test of Significance

Z statistics was applied to determine whether the kappa statistical value for different data set pairs were different, such as single data sets compare with fused data sets and comparison between two fusion data sets.

The results are displayed in Table 11. The difference was considered significant (S) when the Z statistic value surpassed 1.96, for a confidence level of 95%. On the other hand, if the Z value

was lower than 1.96, the discrimination between two classified images was regarded as not significant (NS), for the same confidence level. This table present the value of kappa statistics, the inverse of the square root of the sum of variances for each pair, the value of Z statistic and the confidence level.

Table 11 Test of Significant difference between single data classified images and fused data classified images

Classified Image	$K_1 - K_2$	$1/\sqrt{(\text{Var}_1 + \text{Var}_2)}$	Z Statistic	Confidence Level ($P_{0.05} = 1.96$)
B -- A	0.0568	34.736	1.973	S
I -- A	0.0630	31.937	2.012	S
B -- R	0.2538	20.201	5.127	S
I -- R	0.260	20.146	5.238	S
I -- B	0.0062	42.581	0.264	NS

Note. A- ALOS classified image

R- Radar classified image

B- Brovey Transformation fused classified image

I- IHS Transformation fused classified image

Analysis Table 11 revealed that although the Kappa statistical value of IHS Transformation classified image was higher than Brovey Transformation, the difference between them was not significant. As a result, there was no significant different between the two classified images at a 95% confidence level.

It also could be observed that the classification map of unfused single data sets (ALOS and radar) were significantly different from the fused data sets. In other words, the results of fused data sets performed better than single data sets.

4. Conclusion and Recommendations

4.1. Conclusions

The single ALOS imagery of the whole study area showed the three vegetation communities in red color with different saturation. There were certain divisions between them but not apparent enough. Due to the content of water bodies were different, some lakes in the image were darker than other ones. However, the sand cover type wore a very unique white color which made it easily to be recognized. The classification map of ALOS imagery had the overall accuracy of 88.71%. Three vegetation classes were misclassified in to each other a lot. The water bodies could almost be separated from the original image with only a few misclassifications into other class. The accuracy of sand was very high.

Although filtered by the Gamma MAP filter of the window size 5×5 , the image of ENVISAT Radar looked still noisy. Water bodies in it wore a pure black color, so did the sand covered area. The disparities between *Carex*, *Miscanthus* and *Cynodon* communities were existent but still obscure. The classification result was not so good of radar image. From the classification map we could barely see the separation of three grassland communities. The boundary of water was defined well in the result, however, the sand class was approximately misclassified into water class.

The output of the fused images of optical data set and radar data set show more information (quality of the classification results) of than a single image did. The combined image brought up the differences between the three vegetation communities. Combining the spectral information gained from optical image and complementary information obtained from radar image, the fused images illustrated the three vegetation communities in the much clear belt shape than any of the original single sensor image. Other than the vegetation covered types, the separation between sand, water and hill were bigger than single data set.

The result of Brovey Transformation fused classification map got the overall accuracy of 93.55% and Kappa statistic of 0.9143. Based on comparison with unfused images, the classification results illustrated that, there was significant enhancement in the Brovey fused image classification.

The best result of this research in term of overall accuracy and Kappa statistic were 94.35% and 0.9250 respectively with the fusion method of IHS Transformation. Compare to the other fusion technique Brovey, this one performed slighter better in separate different vegetation communities in classification map. However the difference between them was not significant.

4.2. Implementation

The possibilities of extorting accurate and additional information from image fusion technique proved to be workable and would bring great advantage to the wetland management. Multisensor image fusion techniques in this research provided evidence as a practical tool for updating wetland information about the current status of wetland resources. The accuracy of classification map is significantly increased by image fusion technique. This technique provided a simple, efficient way for the wetland resource inventory.

This study showed the fact that, there major gain in recognition of individual vegetation communities, especially when using the IHS Transformation image fusion technique. By illustrates the current distribution of the wetland vegetation communities which are the reflectance of present condition of wetland resource, this technique could monitor and identify any changes of the vegetation communities. This would be a great help for the local management and they could take actions in time if they need, such as detecting invasive vegetation growing in the wetland or illegal behavior to the wetland and so on.

When analyzed in the suitable regular GIS technique, satellite imagery of adequate information like optical and radar image, could be very useful for further wetland resource management and to prevent the precious area.

4.3. Concluding Remarks

1. Research question 1: What are the different contents of information between ALOS optical and radar in mapping wetland?

Conclusions

The overall accuracies for ALOS and radar classification maps were 88.71% and 75% respectively. The three wetland vegetation communities could be separated in ALOS classification map, although a small part of them was misclassified. And radar data fail to divide them correctly with low accuracy for each of them. Also, the sand class was nearly totally misclassified into water bodies while it could be shown very clearly in ALOS classification map. On the other hand, the water bodies in radar classification map were well defined compare to ALOS.

2. Research Question 2: How accurate is the information extracted from different fusion techniques of radar and optical data used in this research compare to single data sets?

Conclusions

The overall accuracies for fused data were 93.55% (Brovey) and 94.35% (IHS) at the same time as 88.71% (ALOS) and 75% (ENVISAT Radar) for the original data set. The accuracies were significant higher in the fused images. For the three vegetation communities, the producers accuracies raised from 82.29% (ALOS) and 75% (radar) to 92.86% (both fused images) in *Carex*, from 84% (ALOS) and 56% (radar) to 88% (IHS) in *Miscanthus*, from 75% (ALOS) and 62% (radar) to 93.75% (Brovey) in *Cynodon*.

3. Research Question 3: Which fusion technique could best separate and mapping the three wetland vegetation communities well for this research in the study area?

Conclusions

Between the two fusion techniques applied in this research, the IHS Transformation performed slightly better than Brovey Transformation. It was more suitable and appropriate for updating wetland vegetation distribution map for management purpose. However the difference between these two fusion techniques in mapping wetland vegetation communities is not significant.

4.4. Recommendations

The data sets used in this research were one ALOS image and one ENVISAR radar image. For further research, the number and type of both optical and radar data could be increase. It is recommended that other kind of data sets (such as Landsat TM image and other type of radar data) should be considered in order to analysis the fusion technique in a wider degree. The optical image chosen in this study had high quality without any cloudy area. Further research could explore the possibility of multisensor image fusion to minimize or even reduce the cloud effect in optical imagery.

Other than the category of original data set, the other fusion techniques should also be though about in further research. Except the only two fusion methods applied in this study, IHS and Brovey, the possibility of other fusion technique for monitoring and identifying wetland vegetation should be tested as well, such as Principal component analysis and so on.

Further study should be processed using various classification methods like objective oriented classification to discover their capabilities in term of spatial and spectral quality of the original images in increasing the information content for wetland resources management.

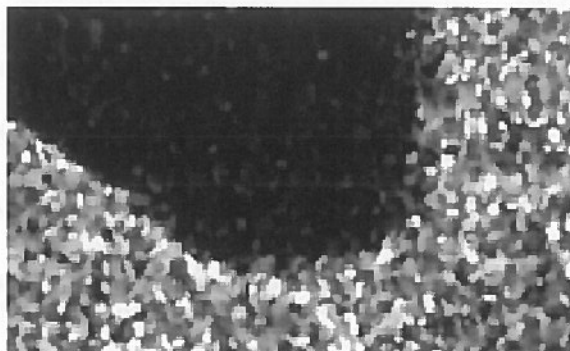
References

- Albertz, J. and R. Tauch (1994). "Mapping from space -- Cartographic applications of satellite image data." *GeoJournal* **32**: 29-37.
- Bakker, W. H., K. A. Grabmaier, G. C. Huurneman, F. D. van der Meer, A. Prakash, K. Tempfli, A. S. M. Gieske, C. A. Hecker, L. L. F. Janssen, G. N. Parodi, C. V. Reeves, M. J. C. Weir, B. G. H. Gorte, J. A. Horn, N. Kerle, C. Pohl, F. J. A. van Ruitenbeek and T. Woldai (2004). *Principles of remote sensing : an introductory textbook*. Enschede, ITC.
- Beaven, S. G., S. Gogineni and F. D. Carsey (1996). "Fusion of satellite active and passive microwave data for sea ice type concentration estimates." *Ieee Transactions on Geoscience and Remote Sensing* **34**(5): 1172-1183.
- Bendjebbour, A., Y. Delignon, L. Fouque, V. Samson and W. Pieczynski (2001). "Multisensor image segmentation using Dempster-Shafer fusion in Markov fields context." *Ieee Transactions on Geoscience and Remote Sensing* **39**(8): 1789-1798.
- Bishop, Y. M., S. E. Fienburg and P. W. Holland (1975). "Discrete multivariate Analysis: Theory and Practicem Cambirdge Massachucetts." MIT Press.
- Bogdanov, A. V., S. Sandven, O. M. Johannessen, V. Y. Alexandrov and L. P. Bobylev (2005). "Multisensor approach to automated classification of sea ice image data." *Ieee Transactions on Geoscience and Remote Sensing* **43**(7): 1648-1664.
- Bruhl, J. J., L. Watson and M. J. Dallwitz (1992). "Genera of Cyperaceae - Interactive Identification and Information-Retrieval." *Taxon* **41**(2): 225-234.
- Cai, S., Y. Ma, H. Zhu and J. Yang (1997). *Poyang Lake typical wetland bio-section monitoring, resource exploration and habitat protection*, Beijing: Science Book Concern.
- Chavez, P. S., S. C. Sides and J. A. Anderson (1991). "Comparison of 3 Different Methods to Merge Multiresolution and Multispectral Data - Landsat Tm and Spot Panchromatic." *Photogrammetric Engineering and Remote Sensing* **57**(3): 295-303.
- Chen, X. (2007). "China Reinforces Wetland Protection." CRI News, from <http://english.cri.cn>.
- Chen, X. L., S. M. Bao, H. Li, X. B. Cai, P. Guo, Z. Y. Wu, W. J. Fu and H. M. Zhao (2007). "LUCC impact on sediment loads in subtropical rainy areas." *Photogrammetric Engineering and Remote Sensing* **73**(3): 319-327.
- Cochran, W. G. (1963). *Sampling techniques*, New York.
- Cohen, J. (1960). "A Coefficient of Agreement for Nominal Scale." *Education and Psychological Measurement*.(20): 37-43.
- Cohen, W. B. and T. A. Spies (1992). "Estimating Structural Attributes of Douglas-Fir Western Hemlock Forest Stands from Landsat and Spot Imagery." *Remote Sensing of Environment* **41**(1): 1-17.
- Congalton, R. G. (2001). "Accuracy assessment and validation of remotely sensed and other spatial information." *International Journal of Wildland Fire* **10**(3-4): 321-328.
- Costa, M. P. F. (2004). "Use of SAR satellites for mapping zonation of vegetation communities in the Amazon floodplain." *International Journal of Remote Sensing* **25**(10): 1817-1835.
- Cracknell, A. P. (1992). "Introduction to Image-Processing - Harrison,Ba, Jupp,Dlb." *International Journal of Geographical Information Systems* **6**(3): 257-257.
- CTAL. (2006). "Wetland Protection." from <http://www.china.org.cn>.
- de Gier, A. (1996). "Sampling Basics." Lecture note, ITC, Enschede, unpublished.
- Dugan, P. J. (1991). "Wetlands, Regional-Planning and the Development Assistance Community." *Landscape and Urban Planning* **20**(1-3): 211-214.
- Everitt, J. H., C. Yang, D. E. Escobar, C. F. Webster, R. I. Lonard and M. R. Davis (1999). "Using remote sensing and spatial information technologies to detect and map two aquatic macrophytes." *Journal of Aquatic Plant Management* **37**: 71-80.
- Franklin, S. E. and C. F. Blodgett (1993). "An Example of Satellite Multisensor Data Fusion." *Computers & Geosciences* **19**(4): 577-583.

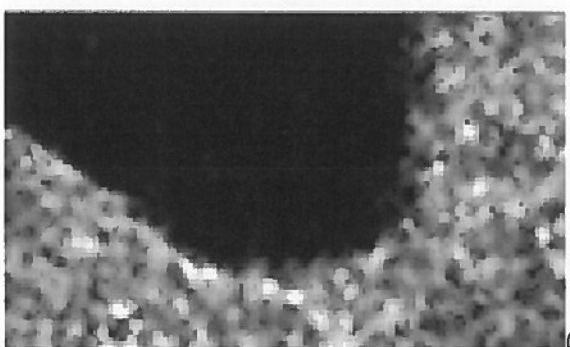
- Genderen, J. L. v. and C. Pohl (1994). "Image Fusion of Optical and Microwave Satellite Data for Earth Science Applications." The UN/ CHINA/ ESA Workshop on Microwave Remote Sensing Applications, Beijing, China 1-7.
- Guan, Y. (2007). Application of MODIS imagery for monitoring dynamics of grassland vegetation in Poyang lake national nature reserve, China. Enschede, ITC: 49.
- Guangmeng, G., C. Yungang and M. Long (2006). "In troduction to ENVISAT-ASAR Data Processing." Remote Sensing Information(4).
- Guo, J. G., A. G. P. Ross, D. D. Lin, G. M. Williams, H. G. Chen, Y. S. Li, G. M. Davis, Z. Feng, D. P. McManus and A. C. Sleight (2001). "A baseline study on the importance of bovines for human Schistosoma japonicum infection around Poyang Lake, China." American Journal of Tropical Medicine and Hygiene 65(4): 272-278.
- Haack, B. and M. Bechdol (2000). "Integrating multisensor data and RADAR texture measures for land cover mapping." Computers & Geosciences 26(4): 411-421.
- Harris, J. R., R. Murray and T. Hirose (1990). "IHS Transform for the Integration of Radar Imagery with Other Remotely Sensed Data." Photogrammetric Engineering and Remote Sensing 56(12): 1631-1641.
- Huang, G. (2006). "On ecological security and ecological construction of Poyang Lake district (in Chinese)." Science & Technology Review 24: 73-78.
- Hussin, Y. A. and S. R. Shaker (1996). "Optical and radar satellite image fusion techniques and their applications in monitoring natural resources and land use changes." Aeu-Archiv Fur Elektronik Und Ubertragungstechnik-International Journal of Electronics and Communications 50(2): 169-176.
- Jiang, Q. H. and D. R. Piperno (1999). "Environmental and archaeological implications of a Late Quaternary palynological sequence, Poyang Lake, southern China." Quaternary Research 52(2): 250-258.
- John, A. R. and J. Xiuping (2006). Remote Sensing Ditital Image Analysis, Birkhäuser.
- Kasischke, E. S. and L. L. BourgeauChavez (1997). "Monitoring South Florida wetlands using ERS-1 SAR imagery." Photogrammetric Engineering and Remote Sensing 63(3): 281-291.
- Kasischke, E. S., K. B. Smith, L. L. Bourgeau-Chavez, E. A. Romanowicz, S. Brunzell and C. J. Richardson (2003). "Effects of seasonal hydrologic patterns in south Florida wetlands on radar backscatter measured from ERS-2 SAR imagery." Remote Sensing of Environment 88(4): 423-441.
- Kuplich, T. M., C. C. Freitas and J. V. Soares (2000). "The study of ERS-1 SAR and Landsat TM synergism for land use classification." International Journal of Remote Sensing 21(10): 2101-2111.
- Lillesand, T. M. and R. W. Kiefer (1994). Remote sensing and image interpretation, Wiley & Sons, New York.
- Ma, Z. and R. L. Redmond (1995). "Tau Coefficients for Accuracy Assesment of Classification of Remote Sensing Data." Photogrammetric Engineering and Remote Sensing(61): 435-439.
- Michelson, D. B., B. M. Liljeberg and P. Pilesjo (2000). "Comparison of algorithms for classifying Swedish landcover using Landsat TM and ERS-1 SAR data." Remote Sensing of Environment 71(1): 1-15.
- Mitsch, W. J. and J. G. Gosselink (2000). "The value of wetlands: importance of scale and landscape setting." Ecological Economics 35(1): 25-33.
- Moreau, S. and T. Le Toan (2003). "Biomass quantification of Andean wetland forages using ERS satellite SAR data for optimizing livestock management." Remote Sensing of Environment 84(4): 477-492.
- Munehika, C. K., J. S. Warnick, C. Salvaggio and J. R. Schott (1993). "Resolution Enhancement of Multispectral Image Data to Improve Classification Accuracy." Photogrammetric Engineering and Remote Sensing 59(1): 67-72.
- Musa, M. K. A. (1999). assessment of multi - data fusion in forest resource management for the Northern part of Selangor, Malaysia. Enschede, ITC: 148.

- Novo, E., M. P. F. Costa, J. E. Mantovani and I. B. T. Lima (2002). "Relationship between macrophyte stand variables and radar backscatter at L and C band, Tucuruí reservoir, Brazil." *International Journal of Remote Sensing* **23**(7): 1241-1260.
- Pasqualini, V., C. Pergent-Martini, G. Pergent, M. Agreil, G. Skoufas, L. Sourbes and A. Tsirika (2005). "Use of SPOT 5 for mapping seagrasses: An application to *Posidonia oceanica*." *Remote Sensing of Environment* **94**(1): 39-45.
- Pohl, C. (1995). SPOT/ERS Image maps: Topographic map updating in Indonesia. SPOT MAGAZINE. **December 1995**: 17-19.
- Pohl, C. and J. L. van Genderen (1998). "Multisensor image fusion in remote sensing: concepts, methods and applications." *International Journal of Remote Sensing* **19**(5): 823-854.
- Sawaya, K. E., L. G. Olmanson, N. J. Heinert, P. L. Brezonik and M. E. Bauer (2003). "Extending satellite remote sensing to local scales: land and water resource monitoring using high-resolution imagery." *Remote Sensing of Environment* **88**(1-2): 144-156.
- Si, Y. (2006). Mapping flood recession grasslands grazed by overwintering geese : an application of multi - temporal remote sensing. Enschede, ITC: 47.
- Silva, T. S. F., M. P. F. Costa, J. M. Melack and E. Novo (2008). "Remote sensing of aquatic vegetation: theory and applications." *Environmental Monitoring and Assessment* **140**(1-3): 131-145.
- Simonit, S., F. Cattaneo and C. Perrings (2005). "Modelling the hydrological externalities of agriculture in wetlands: the case of rice in Esteros del Ibera, Argentina." *Ecological Modelling* **186**(1): 123-141.
- Stehman, S. V. (1997). "Selecting and interpreting measures of thematic classification accuracy." *Remote Sensing of Environment* **62**(1): 77-89.
- Toyra, J., A. Pietroniro, L. W. Martz and T. D. Prowse (2002). "A multi-sensor approach to wetland flood monitoring." *Hydrological Processes* **16**(8): 1569-1581.
- Tung, F. and E. Ledrew (1988). "The Determination of Optimal Threshold Levels for Change Detection Using Various Accuracy Indexes." *Photogrammetric Engineering and Remote Sensing* **54**(10): 1449-1454.
- Tzeng, Y. C. and K. S. Chen (2005). "Image fusion of synthetic aperture radar and optical data for terrain classification with a variance reduction technique." *Optical Engineering* **44**(10): 8.
- Valta-Hulkkonen, K., P. Pellikka, H. Tanskanen, A. Ustinov and A. Sandman (2003). "Digital false colour aerial photographs for discrimination of aquatic macrophyte species." *Aquatic Botany* **75**(1): 71-88.
- Van Gils, H., M. Mwanangi and D. Rugege (2006). "Invasion of an alien shrub across four land management regimes, west of St. Lucia, South Africa." *South African Journal of Science* **102**(9-12).
- Varshney, P. K. (1997). "Multisensor data fusion." *Electronics & Communication Engineering Journal* **9**(6): 245-253.
- Woodcock, C. E., J. B. Collins, S. Gopal, V. D. Jakabhazy, X. W. Li, S. Macomber, S. Ryherd, V. J. Harward, J. Levitan, Y. C. Wu and R. Warbington (1994). "Mapping Forest Vegetation Using Landsat Tm Imagery and a Canopy Reflectance Model." *Remote Sensing of Environment* **50**(3): 240-254.
- Wu, Y. and W. Ji (2002). Study on Jiangxi Poyang Lake national nature reserve., Forest Publishing House, Beijing.
- XNA. (2006). "Wetland." from <http://www.xinhua.org>.
- Zeng, Y. (2006). Monitoring grassland in Poyang natural reserve, China. Enschede, ITC: 44.
- Zhang, L., D. Li, Q. Tong and L. Zheng (1998). "Study of the spectral mixture model of soil and vegetation in PoYang lake area, China." *International Journal of Remote Sensing* **19**(11): 2077-2084.

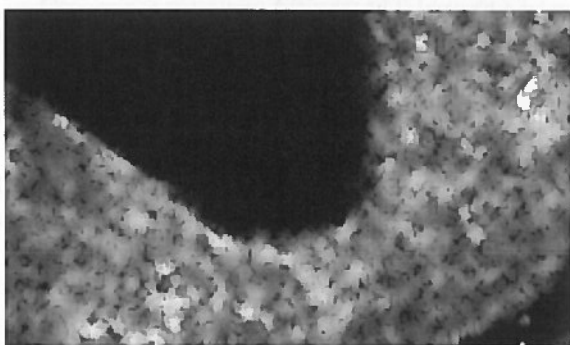
Appendix: Radar filters



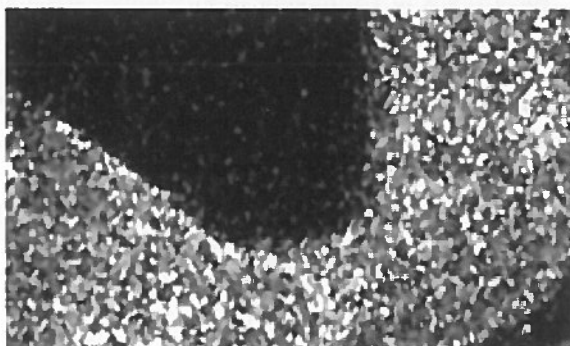
(a).A part of Lee-sigma 3×3 filtered radar image



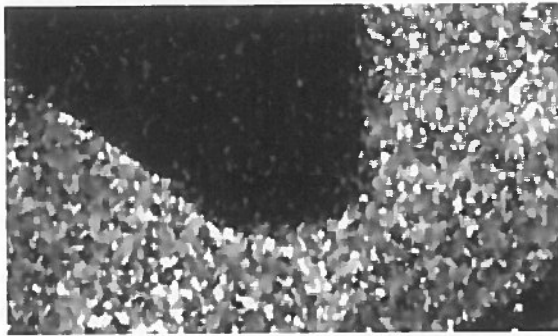
(b).A part of Lee-sigma 5×5 filtered radar image



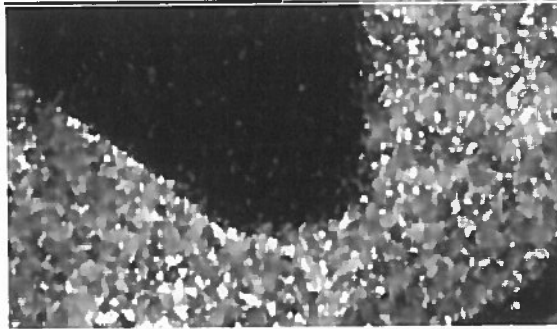
(c).A part of Lee-sigma 7×7 filtered radar image



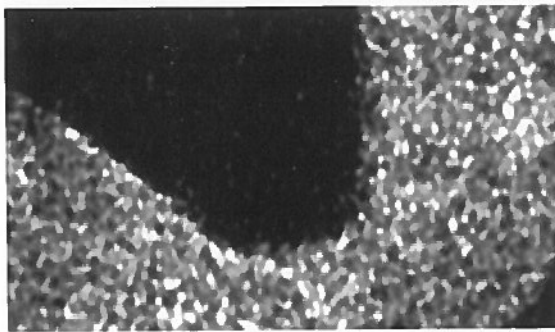
(d).A part of Frost 3×3 filtered radar image



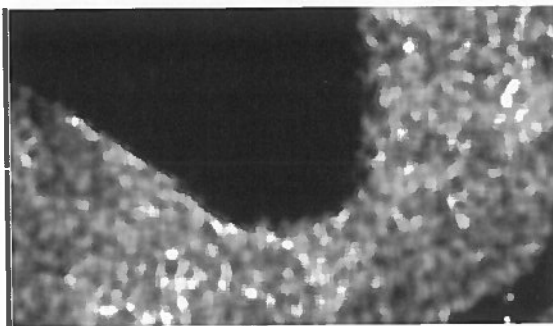
(e).A part of Frost 5×5 filtered radar image



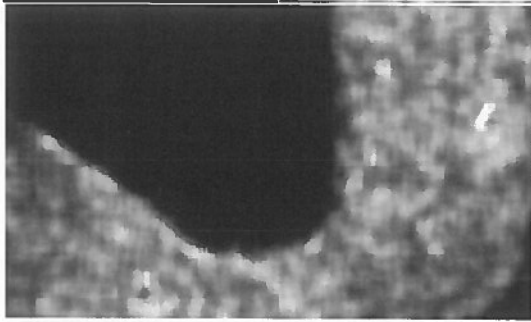
(f).A part of Frost 7×7 filtered radar image



(g).A part of Gamma-MAP 3×3 filtered radar image



(h).A part of Gamma-MAP 5×5 filtered radar image



(i).A part of Gamma-MAP 7×7 filtered radar image

